AEROELASTIC FORMULATION FOR TUNED AND MISTUNED ROTORS

by

EDWARD F. CRAWLEY
Gas Turbine Laboratory
Massachusetts Institute of Technology
Cambridge, Massachusetts

INTRODUCTION

In previous chapters, the analytic tools necessary to approach the problem of aeroelastic analysis have been presented. In the terminology of Bisplinghoff and Ashley (1962), three operators, Inertial, Structural, and Aerodynamic, are needed in the appropriate form. The current state of the art techniques for determining the aerodynamic operators, which are contributed by the unsteady aerodynamicist, have been presented in Chapters 2 through 7. The inertial and structural operators, which together form the structural dynamic model have been reviewed in chapters 12 through 14.

The task of the aeroelastic analysis is to combine the formulations of the structural dynamic and unsteady aerodynamic model in a consistent manner, to solve the resulting aeroelastic model for the desired results (e.g., stability, forced vibration), and to interpret those results for both qualitative trends, and quantitative detail. This task of formulation of the aeroelastic problem and interpretation of the results will be the subject of this chapter.

Specifically, the topics to be addressed are: the formulation of the aeroelastic problem, including a summary of the relations necessary to transform various diverse structural and aerodynamic models to a consistent notation; a brief review of the solution techniques applicable; the trends in aeroelastic stability for tuned rotors; and the effects of mistuning on stability.

In order to understand the motivation for a lengthy discussion of aeroelastic formulations, one must appreciate the challenges and dilemmas faced by the working aeroelastician. First, the starting point of the analysis can vary. Typical starting points can include experimentally or analytically determined mode shapes of the entire blade-disk assembly, mode shapes of individual blades, or the properties of a simple typical section. Secondly, the objective or end point of the analysis may vary. Most often in current practice, a simple assessment of the stability of the turbomachinery stage is desired. Increasingly, however, the full forced vibration response to aerodynamic disturbances is of interest. In principle, the ultimate objective is to develop a completely coupled, time accurate dynamic and aerodynamic model which can be used in such diverse analysis as stall and surge loading, and analysis of mechanical disturbances such as FOD impact, blade loss, rubs, etc. The third challenge facing the working aeroelastician is that all the required analytic tools to progress in an orderly and rigorous manner from the starting point to the end point are not available within the state of the art. For example, a three-dimensional, heavily loaded, large shock motion unsteady aerodynamic operator for the analysis of transonic fan aeroelasticity simply does not exist as of this writing. Therefore existing tools, experimental data and empirical rules must be combined to yield an appropriate engineering solution to the aeroelastic problem.

To illustrate these three problems, varying start points, various goals, and unavailability of analysis tools, consider the very general flow chart for aeroelastic analysis shown in Figure 1. The figure is largely self-explanatory, especially in view of the discussion in earlier chapters, but presents a consistent strategy for combining and extending those topics. What is important to note are the start points, end points, and limitations that prevent full implementation of the charted procedure.

Essentially, three starting points are available, either a structural model of the blade alone, of the nonrotating blade-disk assembly or the rotating blade-disk assembly. In each case, assumed modes, calculated eigenmodes, or measured eigenmodes are possible forms of the starting data. After inclusion of thermal and shaft/rotor support effects, the first possible end point is reached, the rotating natural frequencies, which can be used in traditional Campbell diagram analysis of forced vibration. It is reasonable to say that all of the analytic tools necessary to reach this point on the flowchart are reasonably well developed, and the temporal dependence of the motion can be expressed either in the time or frequency domain. As soon as the next step in the chart is taken, the inclusion of the homogeneous unsteady aerodynamic forces, two limitations appear. First, as has been discussed in Chapters 2 through 7, aerodynamic operators do not exist for all flow regimes, and secondly, intrinsic to the development of these operators is the assumption of sinusoidal motion of the blade row. If the ultimate end point is only the flutter behavior, the assumption of sinusoidal behavior is not limiting, as well known techniques exist for assessing stability even under the assumption of the sinusoidal motion.

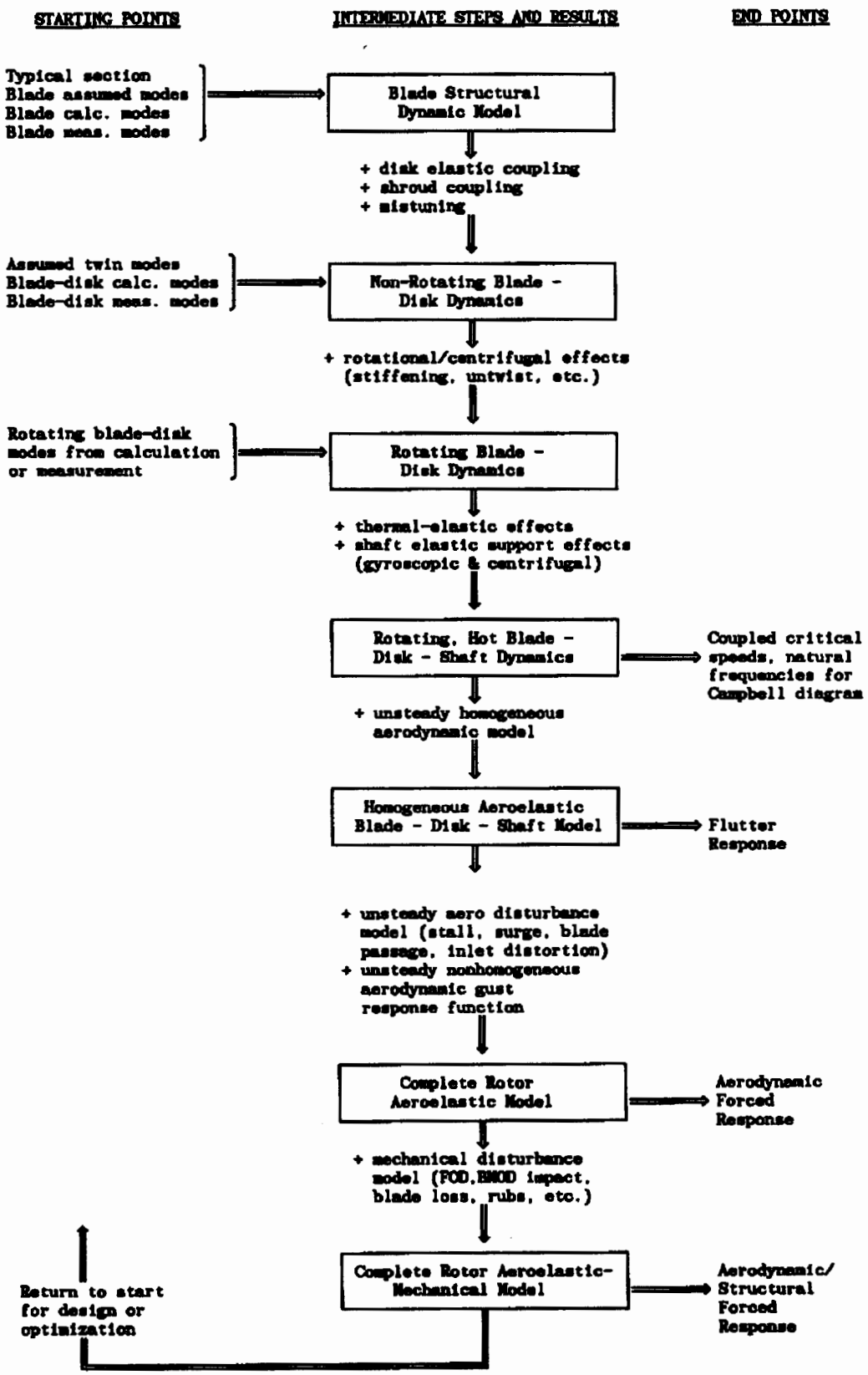

Figure 1. Flowchart for Aeroelastic Analysis

At the next step, however, the addition of the unsteady aerodynamic disturbances and unsteady aerodynamic "gust" response function, even fewer analytic tools are available, and the assumption of sinusoidal motion becomes limiting. Techniques will be presented below to transform the aerodynamic influences derived in the frequency domain, back to the time domain.

Of course, the complete model would include the capability to couple the structural dynamic, aeroelastic and mechanical disturbance models to produce a complete, time accurate model of the turbomachine aeromechanical response. However, due to lack of the proper analytic tools, this is probably not possible at the current time. Ultimately, iteration takes place over this entire procedure, either in the form of heuristic design or formal optimization.

Over the past decade, as the state of the art of aeroelastic analysis has progressed, a number of different formulations of the aeroelastic problems have evolved. These have included travelling wave formulation, individual blade formulations, and standing mode formulations, Kielb and Kaza (1983), Crawley and Hall (1985), Dugundji and Bundas (1984). These formulations have been applied to single and two degree of freedom typical section models, and to blade modal models, Srinivasan (1980), Bendiksen and Friedmann (1981), Srinivasan and Fabunmi (1984). In some models the effect of disk and shroud elastic coupling has also been included, Kielb and Kaza (1984). There has been some doubt as to whether these various formulations are equivalent, and as to which is is most appropriate. One of the objectives of this chapter is to review and summarize these formulations in a consistent notation for single blade degree of freedom analysis, and to show that they are mathematically equivalent. This does not imply that in a given situation one may not be preferred over another due to its ease of application or insight contributed, but merely that simple similarity transforms are available to transform easily from one formulation to another. The direct extension of the one degree of freedom formulation to multiple section or blade modal degrees of freedom is also demonstrated.

In the next section the mathematical formulations and transformations which allow coupling of the various existing analytic tools along the lines of the flowchart of Fig. 1 will be presented.

FORMULATION AND SOLUTION OF THE AEROELASTIC PROBLEM

Basic Relationships

At the foundation of the aeroelastic analysis of turbomachines and propellers are three fundamental relationships: a structural dynamic model of the bladed disk; a kinematic relationship between various expressions for blade motion; and an unsteady aerodynamic model of aerodynamic forces. The most general possible model of the single degree of freedom aeroelastic response of a typical blade section of the ith blade is given as

$$m_i\ddot{q}_i + m_i\omega_i^2 q_i = f_i^m + f_i^D \qquad (1)$$

where m_i is the generalized mass, ω_i its natural frequency, q_i its displacement, f_i^m the motion dependent aerodynamic forces, and f_i^D the aerodynamic disturbance forces acting on the ith blade. When modelling a typical section, the generalized mass and force traditionally have units of mass per span and force per span. The assembly of N structurally uncoupled blades would then be governed by

$$\left[\begin{smallmatrix}\ddots & & \\ & m_i & \\ & & \ddots\end{smallmatrix}\right]\{\ddot{q}_i\} + \left[\begin{smallmatrix}\ddots & & \\ & m_i\omega_i^2 & \\ & & \ddots\end{smallmatrix}\right]\{q_i\} = \{f_i^m\} + \{f_i^D\} \qquad (2)$$

where equation (2) represents N 'independent' equations, which will be recoupled by the motion dependent aerodynamic forces f_i^m. In its most general form, the motion dependent force can be written as

$$\begin{aligned} f_i^m = {} & f_o(q_i, \dot{q}_i, \ddot{q}_i, y_i) + \\ & + f_{+1}(q_{i+1}, \dot{q}_{i+1}, \ddot{q}_{i+1}, y_{i+1}) + \\ & + f_{-1}(q_{i-1}, \dot{q}_{i-1}, \ddot{q}_{i-1}, y_{i-1}) + \\ & + \text{etc.} \end{aligned} \qquad (3)$$

with

$$y_i = \int_o^t \dot{q}_i(\tau) h_o(t-\tau)\,d\tau$$

$$y_{i+1} = \int_o^t \dot{q}_{i+1}(\tau) h_{+1}(t-\tau)\,d\tau$$

$$y_{i-1} = \text{etc...}$$

where, of course, f_o, f_{+1}, f_{-1} depend on the Mach No., reduced frequency, and geometry of the blade and cascade. Equation (3) expresses in a very general way the dependence of the force acting on the ith blade due to its motion and the motion of its neighbors, and on the time history of those motions through lags due to shed vorticity and finite speed of sound. These lag effects are explicitly represented by the augmented state variables y_i.

Unfortunately, within the state of the art, the aerodynamic operators are not available in the very general form of eq. (3). In fact, they are derived for a very specific temporal and spatial motion pattern: sinusoidal in time and fixed interblade phase along the cascade in space. The kinematic relationship between these travelling wave coordinates and the displacement of the i^{th} blade is

$$q_i = \mathrm{Re}\left[\sum_n \bar{q}_{p_n} e^{j(\omega t + i\beta_n)}\right] \qquad (4)$$

where $\bar{q}_{\beta n}$ is the amplitude of the travelling wave of interblade phase β_n $\beta_n = 2\pi n/N$. The sum in n can be taken as

$$n = 0, 1, 2, \cdots, N-1$$

or, equivalently for N an odd number of blades,

$$n = -\frac{(N-1)}{2}, \cdots, -1, 0, 1, \cdots, \frac{(N-1)}{2} \qquad (4a)$$

or, for N an even number of blades,

$$n = -\frac{N}{2} - 1, \cdots, -1, 0, 1, \cdots, \frac{N}{2}$$

since for a rotor of N blades there are N possible interblade phase angles, and small negative angles are equivalent to large positive ones

$$\beta_{-n} = \beta_{N-n} = \frac{2\pi(-n)}{N} \cong 2\pi - \frac{2\pi n}{N} \qquad (4b)$$

It will be convenient to rewrite equation (4) as

$$\{q_i\} = [E]\left\{\bar{q}_{\beta_n}\right\} e^{j\omega t} \qquad (5)$$

$$\text{where } [E] \equiv \begin{bmatrix} E_{0,0} & \cdots & E_{0,N-1} \\ \vdots & & \vdots \\ E_{N-1,0} & \cdots & E_{N-1,N-1} \end{bmatrix} \quad E_{k,\ell} \equiv e^{j\frac{2\pi k\ell}{N}} \qquad (6)$$

The aerodynamic forces per span are usually derived assuming that the blades are undergoing the travelling wave motion of eq. (4), Whitehead (1966), Smith (1972), Adamczyk and Goldstein (1978). Under this assumption the forces per span acting on the zeroth blade undergoing the nth travelling wave, constant interblade phase angle motion of eq. (4) can be expressed as

$$f_o^a = \pi\rho b^2\omega^2 \ell_{\beta_n} \bar{q}_{\beta_n} e^{j\omega t} \qquad (7)$$

where $\bar{q}_{\beta n}$ is the amplitude of the nth travelling wave pattern, and the complex force coefficient due to β_n is $\ell_{\beta n}$.

The force on the i^{th} blade due to the superposition of all the interblade phase angle waves is

$$f_i^a = \pi\rho b^2\omega^2 \sum_{n=0}^{N-1} \ell_{\beta_n} \bar{q}_{\beta_n} e^{j(\omega t + i\beta_n)}$$

$$\text{or} \quad \left\{f_i^a\right\} = \pi\rho b^2\omega^2 [E]\left[\ell_{\beta_n}\right]\left\{\bar{q}_{\beta_n}\right\} e^{j\omega t} \qquad (8)$$

At this point the three fundamental equations of the aeroelastic problem are at hand and will be repeated for clarity. The first is the dynamic governing equation of motion, as would be derived by the structural dynamicist (eq. 2).

$$\left[m_i\right]\{\ddot{q}_i\} + \left[m_i\omega_i^2(1+jg_i)\right]\{q_i\} = \{f_i\} \qquad (9)$$

where the structural damping factor g has been added. The second is the kinematic relationship between individual and traveling wave blade motion (eq. 5)

$$\{q_i\} = [E]\left\{\bar{q}_{\beta_n}\right\} e^{j\omega t} = \left\{\bar{q}_i\right\} e^{j\omega t} \qquad (10)$$

where the last relation simply assumes sinusoidal motion of the individual blades.

The third is the relationship between travelling wave motion and unsteady aerodynamic forces, supplied by the aerodynamicist (eq. 8)

$$\left\{f_i^a\right\} = \pi\rho b^2\omega^2 [E]\left[\ell_{\beta_n}\right]\left\{\bar{q}_{\beta_n}\right\} e^{j\omega t} \qquad (11)$$

These three fundamental relationships can be combined to yield the governing aeroelastic equations in several ways. First, the equations can be expressed in terms of interblade phase angle "modes". This requires transformation of the structural dynamic equation (9) to interblade phase coordinates. Second, the equations can be expressed in terms of individual blade displacements. This requires transformation of the aerodynamic forces, eq. (11) to individual blade coordinates. And third, the equations can be expressed in terms of standing modes of the bladed disk, such as sine and cosine modes, or structural eigenmodes. This requires transformation of both the dynamic equations and aerodynamic forces. Each of those approaches has some value, as will be discussed.

Travelling Wave Formulation

The aeroelastic eigenvalue problem was first formulated in travelling wave coordinates, that is in those coordinates for which the aerodynamic forces are derived, Whitehead (1966). In order to derive the equations in traveling wave coordinates, equations (10) and (11) are substituted into equation (9), giving:

$$-\omega^2\left[m_i\right][E]\left\{\bar{q}_{\beta_n}\right\} e^{j\omega t} + \left[m_i\omega_i^2(1+jg_i)\right][E]\left\{\bar{q}_{\beta_n}\right\} e^{j\omega t} = \pi\rho b^2\omega^2 [E]\left[\ell_{\beta_n}\right]\left\{\bar{q}_{\beta_n}\right\} e^{j\omega t} \qquad (12)$$

premultiplying by E^{-1}, and cancelling the time variation exp(jωt) gives

$$-\omega^2[E]^{-1}\left[m_i\right][E]\left\{\bar{q}_{\beta_n}\right\} + [E]^{-1}\left[m_i\omega_i^2(1+jg_i)\right][E]\left\{\bar{q}_{\beta_n}\right\} = \pi\rho b^2\omega^2\left[\ell_{\beta_n}\right]\left\{\bar{q}_{\beta_n}\right\} \qquad (13)$$

Equation (13) now represents the formulation of the aeroelastic problem in terms of travelling wave coordinates. It has the advantage of using the aerodynamic force coefficients in exactly the form in which they are derived. Furthermore, if the blades have a single degree of freedom and if the blades are uniform in mass and stiffness such that

$$\left[m_i\right] = m[I] \qquad \text{and} \qquad \left[m_i\omega_i^2(1+jg_i)\right] = m\omega_o^2(1+jg)[I] \tag{14}$$

then equation (13) becomes

$$-m\omega^2[I]\left\{\bar{q}_{\beta_n}\right\} + m\omega_o^2(1+jg)[I]\left\{\bar{q}_{\beta_n}\right\} = \pi\rho b^2\omega^2\left[\ell_{\beta_n}\right]\left\{\bar{q}_{\beta_n}\right\} \tag{15}$$

which is the governing homogeneous equation for single degree of freedom flutter for a perfectly tuned rotor. Note that the separate equations in equation (15) are completely uncoupled. This implies that fora tuned rotor, the travelling wave coordinates are the normal aeroelastic eigenmodes, and the eigenvalues associated with each mode are directly related to the unsteady aerodynamic coefficients for that interblade phase angle.

$$-m\omega^2 + m\omega_o^2(1+jg) = \pi\rho b^2\omega^2\ell_{\beta_n} \qquad \text{or} \qquad \omega^2 = \frac{\omega_o^2(1+jg)}{(1+\pi\rho b^2\ell_{\beta_n}/m)} \tag{16}$$

It is an advantageous coincidence that the kinematic assumption of constant interbalde phas travelling wave coordinates made by the unsteady aerodynamicist eventually turn out to be the eigenmodes of the aeroelastic problem for a tuned rotor. The disadvantage of this formulation is that it requires transforming the structural model to travelling wave coordinates, in effect forcing the structural representation into a form chosen for its convenience in the unsteady aerodynamic problem. Although not inconvenient for tuned rotors, transformation of the governing equations to this form makes it very difficult to interpret the aeroelastic response of mistuned rotors with nonuniform blades, and difficult to explicitly include the effects of shroud and disk elastic coupling, Crawley and Hall (1985), Kielb and Kaza (1984). Although the representation of the aerodynamic forces in this form obscures the real physical dependence of forces on specific blade motions, Szechenyi et al (1984), much more insight into these aspects is gained by examining the equations formulated in terms of individual blade coordinates.

Individual Blade Formulation

In order to formulate the problem in terms of individual blade coordinates, the aerodynamic forces must be transformed by substituting equation (10) into equation (11), yielding

$$\{f_i^m\} = \pi\rho b^2\omega^2[L]\left\{\bar{q}_i\right\}e^{j\omega t} \qquad \text{where} \qquad [L] = [E]\left[\ell_{\beta_n}\right][E]^{-1} \tag{17}$$

The flutter equation is found by substituting into equation (9)

$$-\omega^2\left[m_i\right]\left\{\bar{q}_i\right\} + \left[m_i\omega_i^2(1+jg_i)\right]\left\{\bar{q}_i\right\} = \pi\rho b^2\omega^2[L]\left\{\bar{q}_i\right\} \tag{18}$$

which is the aeroelastic equation in terms of individual blade coordinates. The principal advantage of this formulation is that it is expressed in a coordinate system which is a natural one for the structure. Thus, if any complicating features are added to the structure, such as disk elastic coupling, shroud elastic coupling, blade nonuniformity or mistuning, or multiple blade degrees of freedom. This is a simpler starting point for the resulting model than the travelling wave form.

Another advantage of this formulation is that although the aerodynamic coefficients must be transformed into the [L] matrix form, the aerodynamic coefficients as they appear in the [L] matrix give tremendous insight into the unsteady aerodynamic interactions in a cascade. Each term in the aerodynamic influence matrix [L] has a unique physical significance (Fig. 2). The term in the first row and the second column, for example, designates the force acting on the first blade due to the motion of the second blade. By the symmetry of the rotor, assuming that the blades are geometrically identical, this must be the same as the force felt by the second blade due to the motion of the third. Likewise, each term on the diagonal represents the force felt by a blade due to its own motion. The [L] matrix has the form in which there are only N independent complex terms, and the entries of each column are the same, with each column permuted one row relative to the adjacent columns.

$$[L] = \begin{bmatrix} L_o & L_{N-1} & L_{N-2} & \cdots & L_1 \\ L_1 & L_o & L_{N-1} & \cdots & L_2 \\ \vdots & \vdots & \vdots & & \vdots \\ L_{N-1} & L_{N-2} & L_{N-3} & \cdots & L_o \end{bmatrix} \tag{19}$$

The most significant term in [L] is the diagonal term L_o, which expresses the force acting on any given blade due to its own motion, in effect the blade self-stiffness and self-damping. It has been shown that this is the only term in the influence coefficient matrix which can provide a net stabilizing influencing on the rotor, Crawley and Hall (1985), Szechenyi et al (1984).

Mathematically, the individual blade aerodynamic forces L_K are related to the travelling wave forces through a complex Fourier transform relationship

$$L_K = \frac{1}{N}\sum_{n=0}^{N-1} \ell_{\beta_n} \exp\left\{j\frac{2\pi Kn}{N}\right\} \qquad (20)$$

and

$$\ell_{\beta_n} = \sum_{K=0}^{N-1} L_K \exp\left\{-j\frac{2\pi Kn}{N}\right\} \qquad (21)$$

Equation (20) shows that L_k is just the K_{th} coefficient of the discrete Fourier series representation of $\ell_{\beta n}$ given in equation (21). So, for example, if a plot of the aerodynamic coefficients versus β is dominantly the first harmonic of β and an average offset, this implies that [L] is almost tridiagonal, and the physical interpretation is that only the two adjacent blades to a given blade and the blade itself have any direct effect on the blade (Figure 2). If the plot of $\ell_{\beta n}$ vs. β has higher harmonics in β, then the influence of more distant blades is relatively more important.

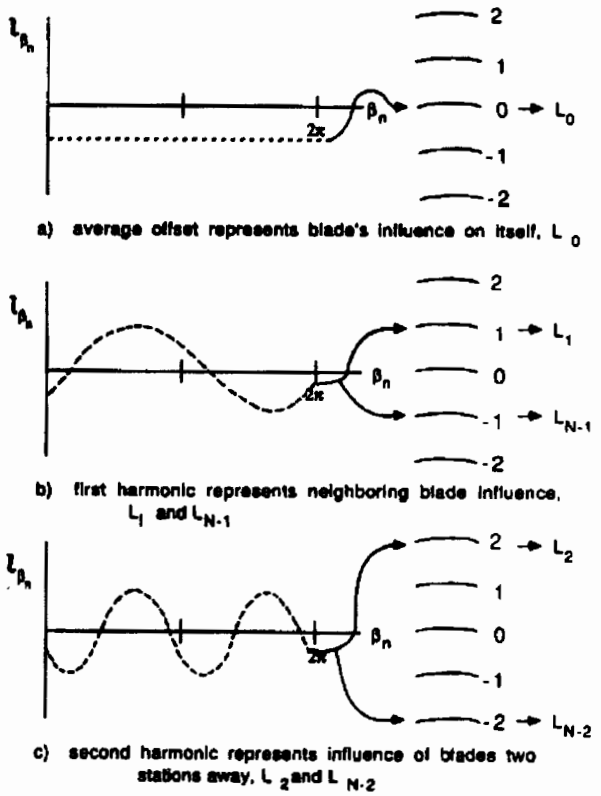

Figure 2. Graphical Relationship Between Aerodynamic Forces in Interblade Phase and Complex Influence Coefficient Form

Standing Mode Formulation

When the starting point of the aeroelastic formulation is a set of calculated or experimentally measured standing structural eigenmodes of the bladed disk assembly, it is desirable to formulate the aeroelastic problem in terms of these modal coordinates, Brooker and Halliwell (1984), Crawley (1983).

If the rotor is tuned, then there will be pairs of repeated structural eigenvalues. In this case, there is not a unique representation of the eigenvectors. Two natural ways to represent the mode shapes are by forward and backward traveling waves, or by sine and cosine standing waves, Dugundji and Bundas (1984). Expressing the motion of the rotor in terms of sine and cosine modes, also known as twin orthogonal modes or multiblade coordinates, gives the representation

$$q_i = b_o + \sum_{n} b_n \cos(n\theta_i) + \sum_{n} a_n \sin(n\theta_i)$$
$$n = 1,2,\cdots,\frac{N-1}{2} \quad \text{for N odd,} \qquad (22)$$
$$n = 1,2,\cdots,\frac{N}{2} \quad \text{for N even,}$$
$$\theta_i = \frac{2\pi i}{N}$$

which still allows arbitraryu time dependence of the motion. If the motion is assumed to be oscillatory, the displacement is

$$\bar{q}_i = \bar{q}_{co} + \sum_{n} \bar{q}_{cn} \cos(n\theta_i) + \sum_{n} \bar{q}_{sn} \sin(n\theta_i) \qquad (23)$$

which can be written

$$\left\{\bar{q}_i\right\} = [P]\begin{bmatrix}\bar{q}_{cn}\\ \bar{q}_{sn}\end{bmatrix} = [P]\begin{bmatrix}\bar{q}_{co}\\ \bar{q}_{c1}\\ \bar{q}_{s1}\\ \bar{q}_{c2}\\ \bar{q}_{s2}\\ \vdots\end{bmatrix} \qquad (24)$$

$$[P] = \begin{bmatrix} C_{0,0} & C_{0,1} & S_{0,1} & C_{0,2} & S_{0,2} & \cdots \\ C_{1,0} & C_{1,1} & S_{1,1} & C_{1,2} & S_{1,2} & \cdots \\ C_{2,0} & \vdots & \vdots & \vdots & \vdots & \\ C_{3,0} & & & & & \\ \vdots & & & & & \\ C_{N-1,0} & \cdots & & & \cdots & S_{N-1,\frac{N-1}{2}} \end{bmatrix} \qquad (25)$$

for N odd

$$C_{k,\ell} = \cos 2\pi\frac{k\ell}{N} \quad \text{and} \quad S_{k,\ell} = \sin 2\pi\frac{k\ell}{N}$$

Since equation (23) expresses the relationship between the individual and sine/cosine modal coordinates, the aeroelastic formulation can be transferred to these coordinates by simply substituting equation (24) into equation (18) and premultiplying by P^{-1} giving

$$-\omega^2[P]^{-1}\left[m_i\right][P]\begin{bmatrix}\bar{q}_{cn}\\ \bar{q}_{sn}\end{bmatrix} + [P]^{-1}\left[m_i\omega_i^2(1+jg_i)\right][P]\begin{bmatrix}\bar{q}_{cn}\\ \bar{q}_{sn}\end{bmatrix} = \pi\rho b^2\omega^2[P]^{-1}[L][P]\begin{bmatrix}\bar{q}_{cn}\\ \bar{q}_{sn}\end{bmatrix} \quad (26)$$

The process of deriving equation (15) from equation (8) is a similarity transform, in which eigenvalues are preserved.

The unique aspect of the pure sine and cosine standing modes is that a pair of like nodal diameter modes can be directly superimposed to form a traveling wave mode. By comparison of equation (10) and equation (24), it can be seen that

$$\left\{\bar{q}_{\beta_n}\right\} = [E]^{-1}[P]\begin{bmatrix}\bar{q}_{cn}\\ \bar{q}_{sn}\end{bmatrix} \quad (27)$$

If the rotor is mistuned, or contains coupled bending torsion motion of the blades, it is no longer simple to relate the standing and travelling waves, but it is still straightforward to relate the standing blade-disk modes to the individual blade deflections. The i^{th} blade deflection is given as

$$q_i = \sum_{n=0}^{N-1}\phi_i^{(n)}q_n \quad (28a)$$

which can be written

$$\{q_i\} = [\phi]\{q_n\} \quad (28b)$$

where ϕ is the matrix whose columns are the traditional structural modes, and q_n are the coordinates of those modes. Comparison of equation (24) and equation (29) show that for perfect sine and cosine twin orthogonal modes that P matrix is just a special case of the normal modal vector matrix ϕ under the assumption of sinusoidal motion.

$$\left\{\bar{q}_i\right\} = [\phi]\left\{\bar{q}_n\right\} \quad (29)$$

and substitution into equation (18) and premultiplication by ϕ^T gives the aeroelastic formulation in terms of arbitrary blade-disk modal coordinates

$$-\omega^2[\phi]^T\left[m_i\right][\phi]\left\{\bar{q}_n\right\} + [\phi]^T\left[m_i\omega_i^2(1+jg_i)\right][\phi]\left\{\bar{q}_n\right\} = \pi\rho b^2\omega^2[\phi]^T[L][\phi]\left\{\bar{q}_n\right\} \quad (30)$$

Note that the left hand side of equation (30) will now be uncoupled, since ϕ are the structural normal modes, but these modes will be aerodynamically coupled by the terms on the right hand side.

The advantage of this formulation is that the starting point is the set of blade disk normal modes, which can incorporate all forms of blade, disk, and shroud elastic coupling. The disadvantage is that the aerodynamic forces in the form in which they appear in equation (30), and the resulting flutter eigenvectors may be difficult to interpret physically.

FORMULATION FOR MULTIPLE SECTION DEGREES OF FREEDOM

So far the various formulations for single blade degree of freeedom flutter have been outlined. However, it is often desirable to include multiple degrees of freedom for each blade in the aeroelastic model, Bendiksen and Friedmann (1980), Kielb and Kaza (1984).

For such a model, such as a bending-torsion coupled typical section analysis, the equations presented above are still valid, but must be generalized appropriately. This generalization process essentially consists of letting each scalar quantity in the equations (9), (10), and (11) take on a sub-matrix nature. The three fundamental relations for one degree of freedom system are summarized here again. The dynamic equation of equilibrium is

$$\left[m_i\right]\{\ddot{q}_i\} + \left[m_i\omega_i^2(1+jg_i)\right]\{q_i\} = \{f_i\} \quad (9)$$

the kinematic relationship between standing and travelling waves is

$$\left\{\bar{q}_i\right\}e^{j\omega t} = [E]\left\{\bar{q}_{\beta_n}\right\}e^{j\omega t} \quad (10)$$

The dependence of the aerodynamic force on motion is

$$\{f_i^m\} = \pi\rho b^2\omega^2[E]\left[\ell_{\beta_n}\right]\left\{\bar{q}_{\beta_n}\right\}e^{j\omega t} \quad (11)$$

If each section is allowed a translational and pitching degree of freedom, then the generalized coordinate sub-matrix map to q_i

$$q_i \longrightarrow \underset{\sim}{q}_i \equiv \begin{bmatrix}h/b\\ \alpha\end{bmatrix}_i \quad (31)$$

where h is the translation of the section, and α is the pitch. The other terms in the equation (9), therefore, map as follows

$$m_i \longrightarrow \underset{\sim}{m}_i \equiv \begin{bmatrix} m & S/b \\ S/b & I/b^2 \end{bmatrix}_i \tag{32}$$

$$m_i\omega_i^2(1+jg_i) \longrightarrow [\underset{\sim}{m}\omega^2(1+jg)]_i \equiv \begin{bmatrix} m\omega_\beta^2(1+jg_\beta) & 0 \\ 0 & \frac{I\omega_T^2}{b^2}(1+jg_T) \end{bmatrix}_i \tag{33}$$

$$f_i \longrightarrow \underset{\sim}{f}_i \equiv \begin{bmatrix} -L/b \\ M/b^2 \end{bmatrix}_i \tag{34}$$

In this typical section analysis all of the generalized mass and force terms are defined on a per unit span basis.

The pitch motion is defined about the elastic axis, such that the stiffness, sub-matrix in equation (33) is diagonal, but the inertia matrix is populated. Note that the usual (unfortunate) aeroelastic convention for positive signs has been used (Figure 3).In modifying the kinematic relationship (equation (10)) the traveling wave coordinates also take on two coordinates for each interblade phase angle

$$q_{\beta_n} \longrightarrow \underset{\sim}{q}_{\beta_n} \equiv \begin{bmatrix} h_{\beta_n}/b \\ \alpha_{\beta_n} \end{bmatrix} \tag{35}$$

The E matrix is now fully populated by sub-matrix blocks

$$E_{k,\ell} \longrightarrow \underset{\sim}{E}_{k,\ell} \equiv \begin{bmatrix} E_{k,\ell} & 0 \\ 0 & E_{k,\ell} \end{bmatrix} \tag{36}$$

so that the E matrix has the form

$$[\underset{\sim}{E}] = \begin{bmatrix} E_{0,0} & 0 & E_{0,1} & 0 & E_{0,2} & 0 & \cdots \\ 0 & E_{0,0} & 0 & E_{0,1} & 0 & E_{0,2} & \cdots \\ E_{1,0} & 0 & \cdots & & & & \\ 0 & E_{1,0} & \cdots & & & & \\ \vdots & \vdots & & & & & \end{bmatrix} \tag{37}$$

Finally, the aerodynamic forces and moments now depend on translation and pitch, so that

$$\underset{\sim}{f}_i \equiv \begin{bmatrix} -L/b \\ M/b^2 \end{bmatrix}_i \tag{38}$$

$$= \begin{bmatrix} \pi\rho b^2\omega^2 \sum_{n=0}^{N-1} \left[\ell_n^{hh} \frac{h_{\beta_n}}{b} + \ell_n^{h\alpha} \alpha_{\beta_n} + \ell_n^{hw} \frac{w_{\beta_n}}{U} \right] e^{j(\omega t + i\beta_n)} \\ \pi\rho b^2\omega^2 \sum_{n=0}^{N-1} \left[\ell_n^{\alpha h} \frac{h_{\beta_n}}{b} + \ell_n^{\alpha\alpha} \alpha_{\beta_n} + \ell_n^{\alpha w} \frac{w_{\beta_n}}{U} \right] e^{j(\omega t + i\beta_n)} \end{bmatrix}$$

where equation (38) includes the effects of impinging wakes of velocity $w_{\beta n}$ and of periodicity β_n being convected into the cascade. Equation (38) can be written

$$\begin{bmatrix} \begin{bmatrix} -L/b \\ M/b^2 \end{bmatrix}_0 \\ \vdots \\ \begin{bmatrix} -L/b \\ M/b^2 \end{bmatrix}_{N-1} \end{bmatrix} = \pi\rho b^2\omega^2 [\underset{\sim}{E}] \left[\underset{\sim}{\ell}_{\beta_n} \right] \left\{ \frac{\underset{\sim}{q}_{\beta_n}}{} \right\} e^{j\omega t} + \pi\rho b^2\omega^2 [\underset{\sim}{E}] \left[\underset{\sim}{\ell}_{w_n} \right] \left\{ \frac{\underset{\sim}{w}_{\beta_n}}{U} \right\} e^{j\omega t} \tag{39}$$

provided E has the definition of equation (37), $q_{\beta n}$ has the definition of equation (35), and ℓ is defined as

$$\underset{\sim}{\ell}_{\beta_n} \equiv \begin{bmatrix} \ell_n^{hh} & \ell_n^{h\alpha} \\ \ell_n^{\alpha h} & \ell_n^{\alpha\alpha} \end{bmatrix} \quad \text{and} \quad \underset{\sim}{\ell}_{w_n} \equiv \begin{bmatrix} \ell_n^{hw} \\ \ell_n^{\alpha w} \end{bmatrix} \tag{40}$$

With these relationships, the bending torsion aeroelastic problem has the same notation as the single degree of freedom problem and all the transformations developed above can be employed. The aeroelastic problem can be formulated in terms of travelling modes, individual blade deflections and standing modes of bending-torsion deflection.

FORMULATION FOR MULTIPLE SPANWISE BLADE MODES

In order to gain a more accurate model of the aeroelastic behavior of a turbomachine component, it is necessary to integrate the unsteady aerodynamic forces over the entire span. Whether two-dimensional strip theory operators (Chapter 3) or a full three-dimensional model is used (Chapters 4 and 5) will depend on the availability and refinement of such operators. The inclusion of spanwiss integration of aerodynamic forces in the aeroelastic formulation is a straightforward extension of the results of the last section. The governing dynamic equation for the i = 0,1,..., N-1 blades is now

$$\left[[\underset{\sim}{M}]_i \right] \left\{ (\ddot{\underset{\sim}{q}}_m)_i \right\} + \left[[K(1+jg)]_i \right] \left\{ (\underset{\sim}{q}_m)_i \right\} = \left\{ (\underset{\sim}{F}_m)_i \right\} \tag{41}$$

with m=1,2,...,M for every i=0,1,...,N-1

where the generalized displacements and generalized forces of the i^{th} blade are now represented at N/2 spanwise stations

$$\{q_m\}_i = \begin{bmatrix} h_1/b \\ \alpha_1 \\ h_2/b \\ \alpha_2 \\ \vdots \\ \alpha_{N/2} \end{bmatrix}_i \qquad \{F_m\}_i = \begin{bmatrix} -L_1\Delta r_1/b \\ M_1\Delta r_1/b^2 \\ -L_2\Delta r_2/b \\ M_2\Delta r_2/b^2 \\ \vdots \\ M_{N/2}\Delta r_{N/2}/b^2 \end{bmatrix}_i \qquad (42)$$

Note that the mass matrix of equation (41) now has units of mass, rather than mass per span, and the other matrices have been redimensioned accordingly. The formulation of equation (41) still assumes that shroudless blades are rigidly fixed to a stiff disk, such that no structural coupling exists between blades.

Rather than solve the coupled structural-aerodynamic problem, the usual procedure is to solve equation (41) for the structural normal modes of the i^{th} blade, (i.e., with f_i set to zero), by solving

$$\underset{N\times N}{[M]_i}\{\ddot{q}_m\}_i + \underset{N\times N}{[K(1+jg)]_i}\{q_m\}_i = 0 \qquad (43)$$

The result of the structural eigenvalue problem for the i^{th} blade is a set of N natural frequencies and mode shapes.

$$\omega_{p_i} \cdot \varphi_i^{(p)} = \begin{bmatrix} h_1/b \\ \alpha_1 \\ h_2/b \\ \alpha_2 \\ \vdots \\ \alpha_{N/2} \end{bmatrix}^{(p)} \qquad p = 1,2,\cdots,N \qquad (44)$$

and an associated set of blade modal coordinates η_{pi} .

In the aeroelastic problem, only a few of the blade modes are generally of interest. Let the number of modes of interest be P, so that the displacement of the ith blade is expressed in terms of P modes

$$\{q_m\}_i = \begin{bmatrix} \varphi^{(1)} & \varphi^{(2)} & \cdots & \varphi^{(P)} \\ \vdots & \vdots & & \vdots \end{bmatrix}_i \begin{bmatrix} \eta_1 \\ \eta_2 \\ \vdots \\ \eta_P \end{bmatrix}_i \qquad (45)$$

and upon substitution into equation (41)

$$\left[\left[M_p\right]_i\right]\left\{\ddot{\eta}_p\right\}_i + \left[\left[\omega^2(1+jg)_p\right]_i\right]\left\{\eta_p\right\}_i = \left\{\{F_p\}_i\right\} \qquad (46)$$

with p=1,2,$\cdots$,P for every i=0,1,$\cdots$,N-1

where the modal mass, modal stiffness, and modal force associated with these P modes are

$$\left[M_p\right]_i \equiv [\varphi^P]_i^T[M]_i[\varphi^P]_i \qquad (47)$$

$$\left[\omega^2(1+jg)_p\right]_i \equiv [\varphi^P]_i^T[K(1+jg)]_i[\varphi^P]_i \qquad (48)$$

$$\{F_p\}_i \equiv [\varphi^P]_i^T\{F_m\}_i \qquad (49)$$

With these definitions the left hand side of equation (46) is completely uncoupled and the mapping of the multiple spanwise blade mode problem to the simple single degree of freedom problem of equation (9), (10), and (11) is possible.

For the displacements, the generalized displacements map to the blade modal coordinates

$$q_i \longrightarrow \{\eta_p\}_i = \begin{bmatrix} \eta_1 \\ \eta_2 \\ \vdots \\ \eta_P \end{bmatrix}_i \qquad (50)$$

for the inertia term the inertia maps to the modal inertia

$$m_i \longrightarrow \left[M_p\right]_i = \begin{bmatrix} M_1 & & & \\ & M_2 & & \\ & & \ddots & \\ & & & M_P \end{bmatrix}_i \qquad (51)$$

and the stiffness terms map to the modal stiffness

$$m_i\omega_i^2(1+jg_i) \longrightarrow \left[\omega^2(1+jg)_p\right]_i = \begin{bmatrix} M_1\omega_1^2(1+jg_1) & & \\ & \ddots & \\ & & M_P\omega_P^2(1+jg_P) \end{bmatrix}_i \qquad (52)$$

and, finally, the blade force f_i maps to the blade modal forces

$$f_i \longrightarrow \{F_p\}_i = \begin{bmatrix} F_1 \\ F_2 \\ \vdots \\ F_P \end{bmatrix}_i \qquad (53)$$

The proper transformation of the blade aerodynamic forces acting on the blade modes is somewhat complex. Careful attention must be paid to keeping track of effects at the same spanwise location around the rotor versus effects along the blade.

When written in the notation of equation (53), the forces acting on the blade modes of the N blades in terms of the motion of the modes of the individual blades is given by equation (54). Note that the form assumes that aerodynamic strip theory has been used. The transformation matrix T is used to change the order of notation for blade degrees of freedom from that used for the structural problem (inner loop on ths blade DoF) to that used in the aerodynamic problem (inner loop on the cascadewise coordinate).

$$\begin{bmatrix} \{F_p\}_{i=0} \\ \{F_p\}_{i=1} \\ \vdots \\ \{F_p\}_{i=N-1} \end{bmatrix} = \pi\rho b^2\omega^2 \begin{bmatrix} [\underset{\sim}{\psi}^P]_{i=0} & & & \\ & [\underset{\sim}{\psi}^P]_{i=1} & & \\ & & \ddots & \\ & & & [\underset{\sim}{\psi}^P]_{i=N-1} \end{bmatrix} \underset{\sim}{T}^T \begin{bmatrix} \Delta r_{m=1}[I] & & & \\ & \Delta r_{m=2}[I] & & \\ & & \ddots & \\ & & & \Delta r_{m=N}[I] \end{bmatrix} \begin{bmatrix} [\underset{\sim}{E}] & & & \\ & [\underset{\sim}{E}] & & \\ & & \ddots & \\ & & & [\underset{\sim}{E}] \end{bmatrix}$$

$$\begin{bmatrix} [\ell_{\beta_n}]_{m=1} & & & \\ & [\ell_{\beta_n}]_{m=2} & & \\ & & \ddots & \\ & & & [\ell_{\beta_n}]_{m=N} \end{bmatrix} \begin{bmatrix} [\underset{\sim}{E}]^{-1} & & & \\ & [\underset{\sim}{E}]^{-1} & & \\ & & \ddots & \\ & & & [\underset{\sim}{E}]^{-1} \end{bmatrix} \underset{\sim}{T} \begin{bmatrix} [\underset{\sim}{\psi}^P]_{i=1} & & & \\ & [\underset{\sim}{\psi}^P]_{i=2} & & \\ & & \ddots & \\ & & & [\underset{\sim}{\psi}^P]_{i=N} \end{bmatrix} \begin{bmatrix} \{\bar{\eta}_p\}_{i=0} \\ \{\bar{\eta}_p\}_{i=1} \\ \vdots \\ \{\bar{\eta}_p\}_{i=N-1} \end{bmatrix} e^{j\omega t} \qquad (54)$$

where the transformation [T] is defined by :

$$\begin{bmatrix} \{q_i\}_{m=1} \\ \{q_i\}_{m=2} \\ \vdots \\ \{q_i\}_{m=N} \end{bmatrix} = [T] \begin{bmatrix} \{q_m\}_{i=0} \\ \{q_m\}_{i=1} \\ \vdots \\ \{q_m\}_{i=N-1} \end{bmatrix}$$

inner loop over i blades

inner loop over m blade stations of the i^{TH} blade

If the aerodynamic forces were derived from a three-dimensional aerodynamic model which assumed a travelling wave pattern of an assumed blade mode shape, then the aerodynamic forces are

$$\{F_p\}_i = \pi\rho b^2\omega^2\Delta r \left[\underset{\sim}{T}\right]\left[\ell_{3\text{-}D}\right]\left[\underset{\sim}{T}\right]^{-1}\{\bar{\eta}_p\}_i e^{j\omega t} \qquad (55)$$

where the $\ell_{3\text{-}D}$ matrix is the representation of travelling wave three-dimensional unsteady aerodynamic forces due to travelling wave motion (Chapters 4 and 5).

It may be desirable to express the aeroelastic equations of motion of a complete rotor in terms of both spanwise blade modes and coupled blade-disk circumferential modes. In this case the formulation for blade modes of his section can be coupled with the formulation for standing blade-disk modes given above to yield the governing equations of motion.

To this point all the necessary transformations and formulations have been rigorously developed to express the spatial (i.e., spanwise and circumferential) dependencies of the aeroelastic formulation. However, the entire formulation to the point, except for the basic equations (3), (4), and (9) have assumed temporally sinusoidal motion. This is due to the assumptions inherent in the derivation of the aerodynamic operators. In the next section, solution techniques for the sinusoidal formulation will be presented, and in the following section, an approximate transformation to an explicit time accurate formulation will be discussed.

SOLUTIONS FOR SINUSOIDAL TEMPORAL REPRESENTATIONS

Under the assumption that the aerodynamic operators are only available for sinusoidal motion, the steps remaining after formulation of the aeroelastic problems are its proper nondimensionalization and solution for stability and forced response. For reference, the dynamic equation of equilibrium, assuming sinusoidal motion is

$$-\omega^2\left[\underset{\sim}{m}_i\right]\{\bar{q}_i\}e^{j\omega t} + \left[\underset{\sim}{m}_i\omega_i^2(1+j\underset{\sim}{g})\right]\{\bar{q}_i\}e^{j\omega t} = \{\underset{\sim}{f}_i\} \quad (56)$$

Generalized forces on the ith blade due to the nth travelling displacement wave pattern and the wake forced vibration terms are

$$\underset{\sim}{f}_i = \pi\rho b^2\omega^2[E]\left[\left[\underset{\sim}{\ell}_{\beta_n}\right]\left\{\bar{q}_{\beta_n}\right\} + \left[\underset{\sim}{\ell}_{w_n}\right]\left\{\frac{\bar{w}_{\beta_n}}{U}\right\}\right]e^{j(\omega t+\beta_n 1)} \quad (57)$$

This will be referred to as the $\underset{\sim}{\ell}$ formulation of aerodynamic forces. Note that the forces are nondimensionalized in time by the square of the frequency of oscillation, and therefore have the form of virtual inertias. A second common form of the aerodynamic operators is (Chapter III)

$$\begin{bmatrix}\tilde{F}\\ \tilde{M}/c\end{bmatrix} = \pi\rho Uc\left[\begin{bmatrix}C_{F_q} & UC_{F_\alpha}\\ C_{M_q} & UC_{M_\alpha}\end{bmatrix}\begin{bmatrix}\tilde{q}_{\beta_n}\\ \tilde{\alpha}_{\beta_n}\end{bmatrix} - \begin{bmatrix}C_{F_w}\\ C_{M_w}\end{bmatrix}\left\{\frac{\tilde{w}}{w}_{\beta_n}\right\}\right]e^{j(\omega t+\beta_n 1)} \quad (58)$$

in which q (unfortunately) stands for the translational velocity, and α for the pitch angle (Fig. 3). If the assumption of sinusoidal motion is made, and the coordinates are assumed to be the translational and pitch displacements, and wake velocity amplitude, then equation (58) can be manipulted to have the form of equation (57).

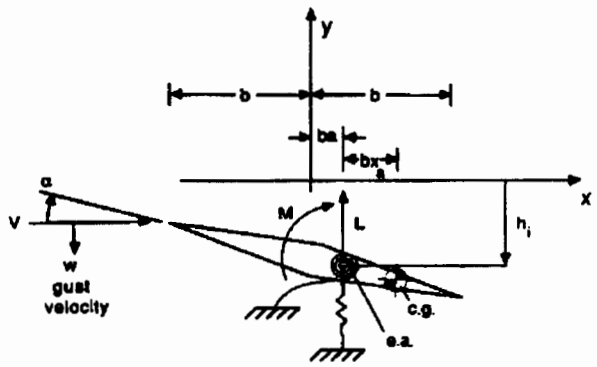

Figure 3a. Notation Convention for 2-dof Model in the $\underset{\sim}{\ell}$ Force Notation

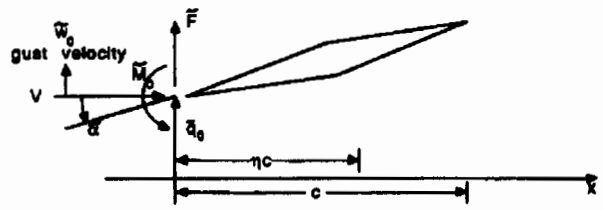

Figure 3b: Notation Convention for the 2-dof Model in the $C_{\underset{\sim}{\ell}}$ Force Notation [Chapter 3]

$$f_i = \begin{bmatrix}-L/b\\ M/b^2\end{bmatrix} \quad (59)$$

$$= \pi\rho U^2\left[\begin{bmatrix}2jkC_{F_q} & 2C_{F_\alpha}\\ 4jkC_{M_q} & 4C_{M_\alpha}\end{bmatrix}\begin{bmatrix}\bar{h}_{\beta_n}\\ \bar{\alpha}_{\beta_n}\end{bmatrix} - \begin{bmatrix}2C_{F_w}\\ 4C_{M_w}\end{bmatrix}\left\{\frac{\bar{w}_{\beta_n}}{U}\right\}\right]e^{j(\omega t+\beta_n)}$$

This will be referred to as the $C_{\underset{\sim}{\ell}}$ formulation for the aerodynamic forces.

If the homogeneous aerodynamic force due to translation and moment due to pitch are examined in the $C_{\underset{\sim}{\ell}}$ form, they are

$$f_i = \frac{-L}{b} = \pi\rho U^2\left[2jkC_{F_q}\right](\bar{h}_{\beta_n}/b) \quad (60)$$

$$f_i = \frac{M}{b^2} = \pi\rho U^2(4C_{M_\alpha})\bar{\alpha}_{\beta_n} \quad (61)$$

In contrast to the $\underset{\sim}{\ell}$ formulation, the aerodynamic forces in the $C_{\underset{\sim}{\ell}}$ formulation are nondimensionalized in time by the square of free stream velocity in the case of the moment (eq. 61), and by the velocity and frequency, in the case of the force, (eq. 60). Therefore these terms appear in the equations of motion as virtual stiffness and damping like terms, respectively. Note that in the $\underset{\sim}{\ell}$ form there is an explicit frequency dependence but no explicit dynamic pressure dependence, whereas in the $C_{\underset{\sim}{\ell}}$ form, there is explicit dynamic pressure dependence, and the explicit frequency dependence is different from that in the former. Thus in comparing reduced frequency dependence of the nondimensional aerodynamic forces, one must keep in mind that the form of the nondimensionalization impacts the apparent trend as the reduced frequency is varied. Of course, as always, one must pay close attention to the sign convention for positive moment and displacement, and for the chord location which is used for the coordinate system reference. A summary of these conventions for the $\underset{\sim}{\ell}$ and $C_{\underset{\sim}{\ell}}$ forms is given in Appendix B. The nondimensionalization and solution techniques will be developed for the simple single degree of freedom equations (9), (10), and (11), since it was shown above that the problems with multiple blade degrees of freedom were simply extensions of the one DoF per blade formulations.

Continuing with only the $\underset{\sim}{\ell}$ form, combinations of eq. (9), (10), and (11) give the aeroelastic problem formulated in individual blade coordinates as

$$-\omega^2\left[\underset{\sim}{m}_i\right]\{\bar{q}_i\} + \left[\underset{\sim}{m}_i\omega_i^2(1+j\underset{\sim}{g}_i)\right]\{\bar{q}_i\} = \pi\rho b^2\omega^2[E]\left[\underset{\sim}{\ell}_{\beta_n}\right][E]^{-1}\{\bar{q}_i\} = \pi\rho b^2\omega^2[L]\{\bar{q}_i\} \quad (62)$$

Division by the blade mass of a section of the nominal blade gives us the nondimensional form of the problem

$$\Omega^2\left[\left[1+\epsilon_i\right] + \frac{1}{\mu}[L]\right]\{\bar{q}_i\} = \left[(1+jg_i)(1+\delta_i)\right]\{\bar{q}_i\} \tag{63}$$

where ϵ_i and δ_i are the fractional mass and stiffness mistuning of the ith blade, Ω is the nondimensional eigenfrequency, $\Omega = \omega/\omega_R$, and μ is the section mass density ratio

$$\mu = \frac{m}{\pi\rho b^2} \tag{64}$$

which premultiplies all of the aerodynamic terms in the governing equations. Note that in the form of equation (64) the mistuning or nonuniformity effects appear explicitly in the formulation.

Equation (63) is of the form of a traditional aeroelastic eigenvalue problem used to determine the stability of the system. The task is to solve for the complex eigenvalues of equation (63). The eigenvalues in general will have a negative real part or a positive real part, indicating mode stability or instability, respectively. The contradiction present in the formulation is, of course, that the system eigenvalues are either exponentially damped or unstable, but in general not purely sinusoidal, while the aerodynamic forces were derived assuming pure sinusoidal motion. Furthermore, these aerodynamic terms depend implicitly on the reduced frequency, but the actual frequency of oscillation is not known until after the eigenvalues are determined.

The traditional solution to this problem is the so-called V-g method, in which the structural damping is assumed uniform, and treated as a free parameter, Bisplinghoff and Ashley (1966). Rewriting equation (63) under these assumptions

$$\left[\left[1+\epsilon_i\right] + \frac{1}{\mu}[L]\right]\{\bar{q}_i\} = \Sigma\left[1+\delta_i\right]\{\bar{q}_i\} \tag{65}$$

where $$\Sigma = \frac{1+jg}{\Omega^2}$$

For a fixed reduced frequency k_R , the eigenvalue problem is then solved for the complex eigenvalues , and for each the frequency of oscillation and damping factor are calculated

$$\Omega = (\mathrm{Re}(\Sigma))^{-1/2}$$
$$g = \mathrm{Im}(\Sigma)/\mathrm{Re}(\Sigma) \tag{66}$$

where g is interpreted as the degree of structural damping necessary to provide neutral (oscillatory) dynamic behavior. The corresponding velocity is then

$$U = \Omega U_R \tag{67}$$

For a N degree of freedom system this will produce N points on the V-g diagram, as shown in Figure 4. By choosing various values of k, families of curves of required damping can be plotted. The stability boundary is then defined as the velocity at which the required damping exceeds the structural damping actually present in the rotor.

Unlike in aeroelastic analysis of aircraft, a key simplification of this process can usually be made for gas turbines. Since the mass ratio is usually large (μ>> 10), the aerodynamic forces are very small compared to the inertial and elastic forces acting on the blade, that is ℓ/μ<< 1. Therefore the oscillatory component of the aeroelastic eigenvalue is usually very close to the reference frequency, implying that the reduced frequency for all of the eigenvalues is very close to the reduced frequency associated with the natural frequency.

This relative weakness of the aerodynamic terms leads to treating equation (63) as a standard eigenvalue problem. That is, a reference value of the reduced frequency is calculated based on the structural frequencies at speed but in vacuum. The aeroelastic eigenvalues are all then calculated and used as is, since little difference between aeroelastic and in vacuum frequency is present.

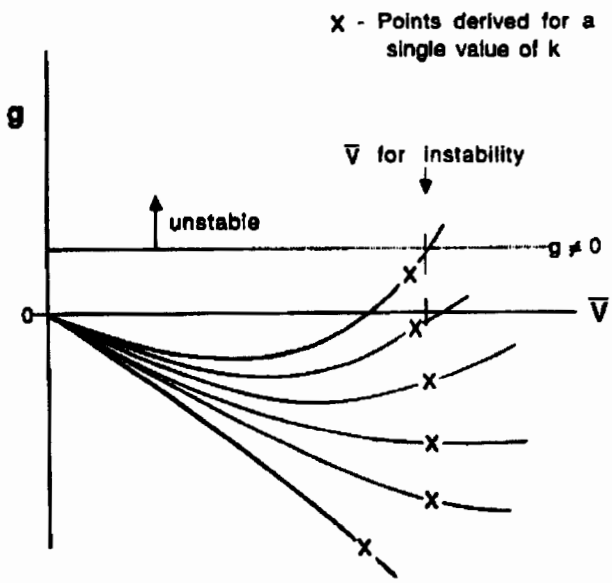

Figure 4: V-g Representation of System Stability

If more accuracy is desired, then two approaches are available. In an iterative approach, after the first calculation, the reduced frequency is modified based upon the calculated oscillatory component of the most critical aeroelastic eigenvalue. This iteration is then continued until the reduced frequency assumed in determining the aerodynamic coefficients, and the calculated reduced frequency of the most critical eigenvalues converge. This procedure resembles the traditional p-k method of aeroelastic analysis.

A second procedure which eliminates the need for this iteration is based on expanding the explicit functional dependence of L on k. If the aeroelastic coefficients are locally fit by a least squares procedure to an expression of the form

$$L(\Omega) = L_o + L_1 \frac{1}{\Omega} + L_2 \frac{1}{\Omega^2} \qquad (68)$$

$$\Omega = \omega/\omega_R = k/k_R$$

Substitution into equation (63) gives a new eigenvalue problem

$$\left[\Omega^2\left[\left\lceil 1+\epsilon_1 \right\rfloor + \frac{1}{\mu}[L]_o\right] + \frac{\Omega}{\mu}[L]_1 + \frac{1}{\mu}[L]_2\right]\{\bar{q}_1\} = \left\lceil (1+jg_1)(1+\delta_1) \right\rfloor \{\bar{q}_1\} \qquad (69)$$

which can be rewritten as a standard eigenvalue problem and solved directly for the aeroelastic eigenvalues.

The results of these formulations are aeroelastic eigenvalues which can be plotted in the complex plane. If the traditional complex s-plane interpretation is desired, then the plot must be of

$$s = j\Omega \qquad (70)$$

as shown in Figure 5a for a single value of reduced frequency k. If a range of k is plotted, the root locus of the individual eigenvalues plot out as curves originating at $(0 + 1_j)$ in the case of no structural damping. Instability is then defined to occur as the first root crosses into the right half planes (Fig. 5b).

There remains in all this analysis the contradiction that the system behavior is non-oscillatory, while the aero forces were derived for oscillatory behavior. Where accuracy is most needed, at the point of neutral stability, the behavior is truly oscillatory, so the aerodynamic forces are exact. Common sense would dictate that for lightly damped and marginally unstable systems, the stability margin would approximate the true damping ratio of the system. This, in fact, has been shown to be the case, but a proof requires the expression of the aerodynamic forces in time explicit form, Dugundji and Bundas (1984). An approximate scheme for this time accurate representation will be shown in the next section.

EXPLICIT TIME DEPENDENT FORMULATION OF AERODYNAMIC FORCES

While sinusoidal representation of motion is adequate for stability analysis, it is sometimes desirable to express the aeroelastic equations of motion with explicit time dependence of the unsteady aerodynamic terms. Examples of when this might be needed are when the excitation or response is expected to differ from a sinusoidal behavior. Such non-sinusoidal behavior occurs in certain forced vibration phenomena, such as impacting or mechanical rubs, and time unsteady aero disturbances, such as rotating stall and surge. Furthermore, whenever time marching calculations are to be done, it will be necessary to have the aerodynamic forces in a time domain representation.

Unfortunately, the unsteady aerodynamic operators have been derived assuming sinusoidal behavior in time and travelling wave constant interblade phase angle in space. In the special transformations above, a complex inverse discrete Fourier transform (eq. 17) was used to remove the restriction of assumed travelling waves, and to express the aerodynamic forces in terms of the individual blade motions. The resulting form was

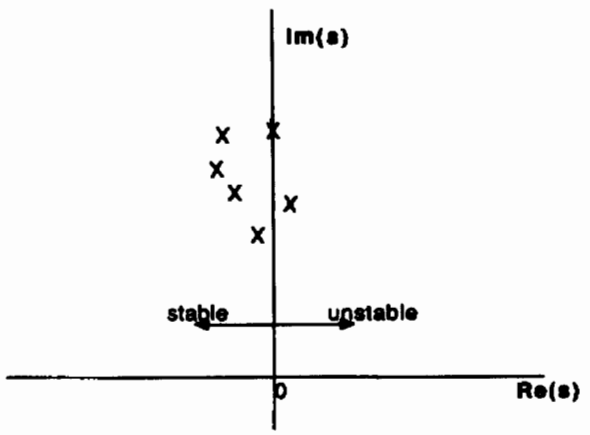

Figure 5a: Complex s-Plane Interpretation of Aeroelastic Eigenvalues for a Single k

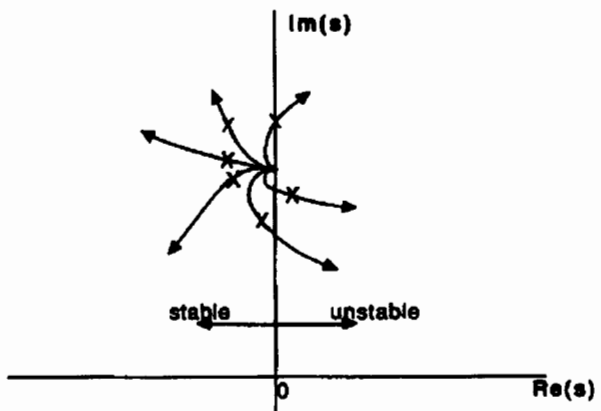

Figure 5b: Complex s-Plane Interpretation of Eigenvalue Root Loci for Increasing k

$$\{f_1\} = \pi\rho b^2\omega^2[L]\left\{\bar{q}_1\right\}e^{j\omega t} \qquad (71)$$

where each column of L was identical, and shifted down one row relative to its neighbor. Thus all the diagonal terms are L_o , the blade's aerodynamic force on itself, the first diagonal below the principal is L_1 , the effect of the adjacent blade downstream, etc. (eq. 19). The elements of the matrix L are of course complex and functions of the reduced frequency k. The restriction of sinusoidal temporal behavior was therefore still present.

In principle, a complex inverse Fourier integral in the reduced frequency parameter k, allowing k to range from zero to infinity, could be taken of the elements of L in order to explicitly transform them to the time domain. In practice, the frequency dependence of the L terms is either expressed as a very complicated expression of k, or, if L is found through computational techniques, never written as an analytic function of k. Thus approximate transform techniques from the frequency to time domain must be used.

The most popular approximate transform technique for unsteady aerodynamic forces involves the so-called Pade approximation of exponential lags in the aerodynamic forces, Edwards et al. (1979). In order to prepare the aerodynamic coefficients for this approximation procedure, it is necessary to convert the coefficients to a form in which the frequency does not appear explicitly in the nondimensionalization

$$\{f_1\} = \pi\rho U^2\left[\frac{b^2\omega^2}{U^2}[L]\right]\left\{\bar{q}_1\right\}e^{j\omega t} = \pi\rho U^2[C]_L\left\{\bar{q}_1\right\}e^{j\omega t} \qquad (72)$$

where $[C]_L = k^2[L]$

The c_L form of the coefficients is similar, but not identical to the c_ℓ form. Now a general approximation to the time dependent form of the aerodynamic forces is introduced

$$\{f_1\} = \pi\rho U^2\left[\frac{b^2}{U^2}[C]_2\{\ddot{q}_1\} + \frac{b}{U}[C]_1\{\dot{q}_1\} + [C]_o\{q_1\} + \left[\;\right]\left\{y_1^{(o)}\right\} + \left[\;\right]\left\{y_1^{(1)}\right\} + \left[\;\right]\left\{y_1^{(2)}\right\} + \cdots\right] \qquad (73)$$

$[G]_o \qquad [G]_1 \qquad [G]_2$

where C_2 , C_1 and C_0 are real circulant matrices of the same form as L (i.e., only N unknowns, all columns identical but shifted). The matrices C_2 , C_1 , and C_0 represent the inertial, damping, and stiffness effects of the aerodynamics. The matrices G_o, G_1, G_2, etc. are sparse real circulant matrices with only one entry per column. They contain the impact of the relative lags in the aerodynamics on the blade forces. G_j, for example, contains the coefficient which expresses the lagged forces of the i+j blade on the i blade.

The vectors of y_i are augmented states, related to q_i by

$$\frac{b}{U}\dot{y}_i^{(\ell)} + g_\ell y_i^{(\ell)} = \frac{b}{U}\dot{q}_i \quad \begin{matrix}\text{for } i=0,1,\cdots,N-1 \\ \text{and } \ell=0,1,\cdots,N-1\end{matrix} \qquad (74)$$

In other words, the y_i variable is a first order lag of time constant g_ℓ, on the rate of change of the displacement q_i. The time constants are the same for all the nominally identical blades. Such approximations are motivated by their success in approximately unsteady aerodynamic forces in external flows and cascades.

In order to evaluate the unknown constants in C_2, C_1, C_0, G_o, G_1 etc., equations (73) and (74) are expanded to examine the forces acting on the zeroth blade. Equation (73) gives

$$f_o = \pi\rho bU^2\left[\frac{b^2}{U^2}(C_{0,2}\ddot{q}_o + C_{1,2}\ddot{q}_1 + \cdots + C_{N-1,2}\ddot{q}_{N-1}) + \frac{b}{U}(C_{0,1}\dot{q}_o + C_{1,1}\dot{q}_1 + \cdots + C_{N-1,1}\dot{q}_{N-1}) + (C_{0,0}q_o + C_{1,0}q_1 + \cdots + C_{N-1,0}q_{N-1}) + (G_{o,o}y_o^{(o)} + G_{1,1}y_1^{(1)} + \cdots + G_{N-1,N-1}y_{N-1}^{(N-1)})\right] \qquad (75)$$

$$\frac{b}{U}\dot{y}_i^{(\ell)} + g_\ell y_i^{(\ell)} = \frac{b}{U}\dot{q}_i \quad \begin{matrix}\text{for } i=0,1,\cdots,N-1 \\ \text{and } \ell=0,1,\cdots,N-1\end{matrix} \qquad (76)$$

Assuming pure sinusoidal motion

$$\{q_1\} = \left\{\bar{q}_1\right\}e^{j\omega t} \qquad (77)$$

then substitution into equations (75) and (76), and combining the two, the force on the zeroth blade can be written

$$f_o = \pi\rho U^2\left\{\left[-k^2C_{0,2} + jkC_{0,1} + C_{0,0} + G_{0,0}\frac{k^2+jkg_o}{g_o^2+k^2}\right]\bar{q}_o e^{j\omega t} + \left[-k^2C_{1,2} + jkC_{1,1} + C_{1,0} + G_{1,1}\frac{k^2+jkg_1}{g_1^2+k^2}\right]\bar{q}_1 e^{j\omega t} + \cdots\right. \qquad (78)$$

If equation (72) is expanded in a manner similar to equation (78), then the force on the zeroth blade is

$$f_o = \pi\rho U^2\left\{\left[\mathrm{Re}(C_{L_o}) + j\mathrm{Im}(C_{L_o})\right]\bar{q}_o e^{j\omega t} + \left[\mathrm{Re}(C_{L_1}) + j\mathrm{Im}(C_{L_1})\right]\bar{q}_1 e^{j\omega t} + \cdots\right. \qquad (79)$$

By comparing equations (78) and (79) term by term, the following relations are apparent

$$-k^2 C_{r,2} + C_{r,0} + C_{r,r}\frac{k^2}{g_r^2+k^2} = \mathrm{Re}(C_{L_r}) \qquad (80)$$

$$kC_{r,1} + C_{r,r}\frac{kg_r}{g_r^2+k^2} = \mathrm{Im}(C_{L_r}) \qquad r=0,1,\cdots,N-1$$

where the C's, G's, and g's are real constants to be determined, and C_{Lr} is a complex function of k.

All that remains is for the real unknowns to be determined by a fitting procedure, such as a least squares fit to C_{Lr} versus the reduced frequency k for each value of the index r. Such experience in fitting sometimes produces an adequate fit using the single lag pole shown. This is true for the case of an incompressible cascade, Dugundji and Bundas (1984). More accuracy is attained by introducing a second set of poles g' and associated constants G'. The classic Jones approximation to the Theodorsen function is an example of this kind of two pole fit, Bisplinghoff and Ashley (1962).

Once the aerodynamic constants have been determined, the governing equation of equilibrium, equation (9),and the time domain expression for the aerodynamic forces can be combined into a single expression.

$$\left[m_1\right]\{\ddot{q}_1\} + \left[m_1\omega_1^2(1+jg_1)\right]\{q_1\} =$$

$$\pi\rho U^2\left[\frac{b^2}{U^2}[C]_2\{\ddot{q}_1\} + \frac{b}{U}[C]_1\{\dot{q}_1\} + [C]_0\{q_1\}\right.$$

$$\left.[C]_0\left\{y_1^{(0)}\right\} + [C]_1\left\{y_1^{(1)}\right\} + [C]_2\left\{y_1^{(2)}\right\} + \cdots\right] \qquad (81)$$

$$\text{where } \frac{b}{U}\left\{\dot{y}_1^{(\ell)}\right\} + \left[g_\ell\right]\left\{y_1^{(\ell)}\right\} = \frac{b}{U}\{\dot{q}_1\}$$

$$\ell = 0,1,\cdots,N-1$$

If a similar procedure is used to represent the unsteady wake or gust response function, then a complete time accurate time domain representation of the aeroelastic behavior can be achieved.

TRENDS IN AEROELASTIC STABILITY

As with many engineering analyses, there are certain dominant trends in the analysis of the aeroelastic stability of turbomachine rotors. Some, such as the role of the mass ratio or the importance of blade mistuning can be determined simply from careful examination of the governing equations. Others require solutions for ranges of parameters to determine overall trends. In this section four trends will be addressed: the stabilizing and destabilizing influences in a cascade, and the critical role of the blade self-damping; the effects of bending-torsion coupling; the real rotor effects of loading, three-dimensionality and stall; and the differences in analysis of actual rotors and "rubber" designs.

Stabilizing and Destabilizing Influences in Cascades.

Simply from examination of the stability eigenvalue problem, certain stabilizing and destabilizing effects can be identified for a single degree of freedom flutter model. The nondimensional form of the stability problem, equation (63), is

$$\frac{1}{\Omega^2}\left[(1+jg_1)(1+\delta_1)\right]\{\bar{q}_1\} = \left[\left[1+\epsilon_1\right] + \frac{1}{\mu}[L]\right]\{\bar{q}_1\} \qquad (82)$$

in which g is the structural damping δ, and ϵ the stiffness and mass nonuniformity, and L, the complex aerodynamic influence coefficients of the form

$$[L] = \begin{bmatrix} L_0 & L_{N-1} & L_{N-2} & \cdots & L_1 \\ L_1 & L_0 & L_{N-1} & \cdots & L_2 \\ L_2 & L_1 & L_0 & \cdots & L_3 \\ \vdots & \vdots & \vdots & & \vdots \\ L_{N-1} & L_{N-2} & L_{N-3} & \cdots & L_0 \end{bmatrix} \qquad (83)$$

In order to identify the stabilizing and destabilizing influences, we simplify the problem by allowing the blades to be uniform in stiffness and structural damping. The governing equations for one degree of freedom per blade flutter are then

$$\frac{1}{\Omega^2}\{\bar{q}_1\} = \frac{1-jg}{1+g^2}\left[\left[1+\epsilon_1\right] + \frac{1}{\mu}[L]\right]\{\bar{q}_1\} \qquad (84)$$

The remaining parameters in the problem are the structural damping g, the mass mistuning ϵ_i , the mass ratio μ , and aerodynamic coefficients L_0 through L_N . Each of these terms somehow influences the eigenvalues Ω .

The complex eigenvalues of equation (84) form a pattern in the s-plane, with $s = j\Omega$, as shown in Figure 6. This pattern can be considered to have a centroid, and the eigenvalues are distributed about this centroid.

The location of the centroid is critical to the stability. If the centroid is in the right half plane, then by definition some eigenvalues will be in the right half plane, and the system will be unstable. Thus, to assure system stability the centroid must be in the left half plane. Returning to equation (84), it has been shown, Crawley and Hall (1985), that the only terms which can exert a net stabilizing influence on the rotor are the structural damping g, and the term L_0, which expresses the aerodynamic force felt on the blade due to its own motion. To show the importance of this term, consider the problem of equation (84). Making use of the matrix property that the sum of the eigenvalues of a matrix equals the trace of the matrix, we have the following relationship for the sum of the eigenvalues:

$$\frac{1}{N}\sum_{k=0}^{N-1}\frac{1}{\Omega_k^2} = \left[1 + \frac{L_0}{\mu} + \frac{1}{N}\sum_{i=0}^{N-1}\epsilon_i\right]\left[\frac{1-ig}{1+g^2}\right] \qquad (85)$$

In the absence of unsteady aerodynamic forces, the reference blade vibrates at at the nondimensional eigenfrequency $\Omega = \Omega_R = 1$. In the presence of aerodynamic forces, which are small compared to the elastic and inertial moments, Ω will still be nearly equal to Ω_R. The eigenfrequency can be expressed as a sum of its reference value and a perturbation from the reference value Ω_R.

$$\Omega = \Omega_R + \tilde{\Omega} = 1 + \tilde{\Omega} \qquad (86)$$

The last step in eq. (86) is due to Ω_R being unity (see Eq. 68). Hence the eigenvalues of eq. (85) can be expanded as

$$\frac{1}{\Omega^2} = \frac{1}{1 + 2\tilde{\Omega} + \tilde{\Omega}^2} = 1 - 2\tilde{\Omega} + O(\tilde{\Omega}^2) \qquad (87)$$

For convenience, let $s = \Omega j$. Substitution of eq. (87) into eq. (85) yields that the centroid of the eigenvalues (Fig. 6) is given approximately by

$$\begin{aligned} \mathrm{Re}\langle s\rangle &= \frac{1}{2}\mathrm{Im}\left[\frac{L_0}{\mu}\right] - \frac{1}{2}g \\ \mathrm{Im}\langle s\rangle &= 1 - \frac{1}{2}\mathrm{Re}\left[\frac{L_0}{\mu}\right] - \frac{\langle\epsilon\rangle}{2} \end{aligned} \qquad (88)$$

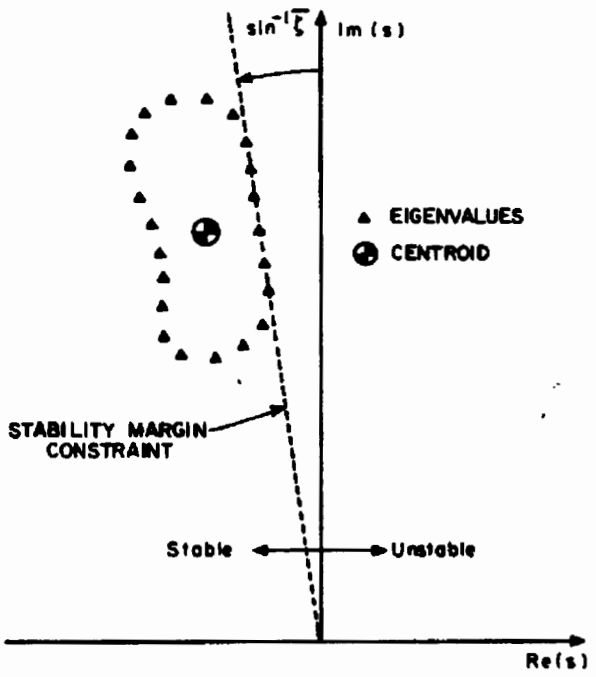

Figure 6. s-Plane Interpretation of Eigenvalues Showing Centroid and Stability Margin Constraint

That is, in the absence of structural damping, the real part of the centroid, $\langle s\rangle$, depends on the imaginary part of L_0, and the structural damping g. The imaginary part of the centroid depends on the real part of L_0 and the mean value of the mistuning.

The location of the eigenvalues in the s-plane can be considered to be distributed around the centroid. Recalling that the system will be unstable if any eigenvalue is in the right half plane, the objective is to assure that the least stable eigenvalue is as far to the left as possible. If the rotor is unstable, increases in stability can be achieved either by moving the centroid to the left, or by reducing the size of the distribution about the centroid, which pulls the rightmost eigenvalue to the left.

Interpreted in this light, eq. (88) is an important result. It shows that in the absence of structural damping the centroid of the eigenvalues lies in the left plane if and only if $\mathrm{Im}(L_0)$ is less than zero. Since a necessary condition for aeroelastic stability of the rotor is that the centroid of the eigenvalues lies in the left half plane, it can be deduced that a necessary but not sufficient condition for stability is that $\mathrm{Im}(L_0)$ be less than zero. This is equivalent to the condition that the blades be self damped.

The location of the centroid is set by the average value of the mass (and stiffness) of the blades, the structural damping, and the blade self damping term. The distribution of the eigenvalues about the centroid is controlled by the nonuniformity in the mass and stiffness and by the off-diagonal terms in the aerodynamic influence coefficient matrix equation (83) (i.e., the unsteady cascade influences in the aerodynamics).

Note that any amount of off-diagonal aerodynamic influence, that is any unsteady aerodynamics effects due to neighboring blades, will distribute the eigenvalues about the centroid, and therefore move some of the eigenvalues to the right, destabilizing the cascade. Thus, unsteady aerodynamic interactions amongst the blades in a cascade are destabilizing.

The distribution pattern of eigenvalues about the centroid is influenced by the pattern of stiffness and mass mistuning of the blades, but the location of the centroid is not influenced by the pattern of mistuning so long as the average value is zero. Thus, the effect of mistuning is to reduce the influence of the blade to blade aerodynamic coupling and move the less stable eigenvalues toward the centroid. Note that no amount of mistuning will cause the centroid to move in a stabilizing direction and no amount of mistuning can increase the stability margin of the rotor beyond that given by the blade self damping.

Finally, the importance of the mass ratio and structural damping can be seen for a one degree of freedom flutter by examining equations (84) and (88). It is clear that all of the aerodynamic influences are scaled by the mass density ratio. In particular, if a necessary stability criterion is that the centroid of the eigenvalues is in the left-half plane then for stability

$$\begin{aligned} &\mathrm{Re}\langle s\rangle \leq 0 \\ &\mathrm{Im}\left[\frac{L_Q}{\mu}\right] - g \leq 0 \end{aligned} \qquad (89)$$

A similar relationship is derived from the previous tuned rotor analysis in which a sufficient condition for stability of a tuned rotor was that

$$\mathrm{Im}\left[\frac{\ell_{\beta_n}}{\mu}\right] - g \leq 0 \qquad (90)$$

for the largest positive value of the aerodynamic coefficient $\ell_{\beta n}$. In each of these cases, the relative contribution of the aerodynamic component and structural damping is scaled by the mass density ratio μ.

In the limiting case of no structural damping, the stability boundary is independent of the mass ratio, since even a small amount of destabilizing aerodynamic influence will cause the rotor to go unstable. However, in the presence of a fixed nonzero structural damping ratio, the mass ratio sets the magnitude of destabilizing aerodynamic effect which can be tolerated before the system becomes unstable. If the rotor speed is increased past the reduced velocity corresponding to neutral aerodynamic stability for a fixed structural frequency and damping, a rotor blade with a larger mass ratio will be more stable than a rotor with a smaller mass ratio, as shown in Figure 7. The mass ratio of course can be changed by either changing the gas density, or by a change in the blade material.

The stabilizing and destabilizing effects for a single degree of freedom flutter model can be summarized as follows:

1. In the absence of structural damping, the blade must be self damped, so that the centroid of the eigenvalues lies in the left half plane.

2. In the presence of structural damping, blades of larger mass ratio are relatively more stable than those of smaller mass ratio for the same damping g.

3. The cascade unsteady aerodynamic influences are destabilizing.

4. Structural mistuning does not change the location of the centroid, but can rearrange the eigenvalues to increase the stability of the least stable root. The limit to the potential effectiveness of mistuning is the centroid of the eigenvalues of the tuned rotor.

While these four trends are rigously true for single degree of freedom per blade flutter, they are generally applicable to any turbomachine in which the flutter dominantly involves a single degree of freedom per blade. This is generally true of solid metallic blades. In the case of hollow or composite blades with significant bending torsion coupling, more judgment should be used in interpreting these stablizing and destablizing cascade influences.

Bending-Torsion Coupling

Several authors have investigated the impact of modeling cascade flutter as a classical bending-torsion coupled problem. In order to not confuse issues, two distinct mechanisms of bending-torsion coupling must be distinguished:

A. Single mode coupling -this occurs when a single torsional mode has some translational component, or a single bending mode has some torsional component. Although its origin may be dynamic, this is essentially a kinematic coupling. It may be due to the root not being supported along a line normal to the elastic axis (i.e., structural sweep), the presence of an offset between the elastic axis and center of mass, the presence of anisotropic materials or fibers, or the presence of shrouds at tip or midspan;

B. Dynamic coupling between two modes - which is the case when two independent modes dynamically interact to cause a classic bending-torsion like coalescence flutter.

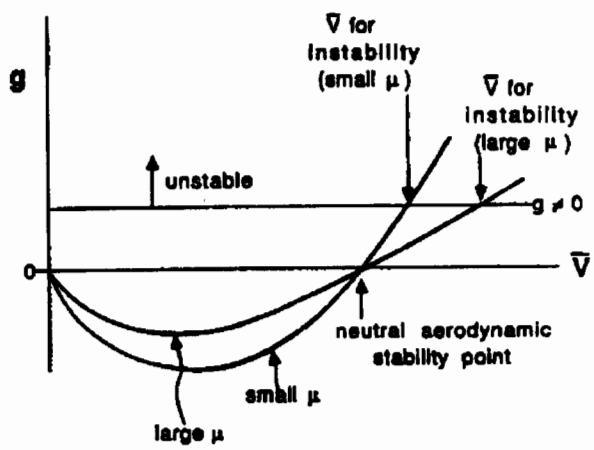

Figure 7: Sensitivity of Rotor Stability to Mass Ratio for Single Degree of Freedom Flutter

In considering the effect of mistuning on stability, one must understand the mechanisms of mistuning; that is, what physical effects cause a change in stability. The auxiliary questions are then: how much mistuning must be present to consider a rotor mistuned; how much change in stability margin can be achieved by mistuning; what is the optimal pattern of mistuning; and what are the limitations to mistuning for stability augmentation.

When deliberately introducing mistuning for stability, one would like to pick an arrangement of mistuning which provides a large increase in stability for a given level of structural mistuning. It has been suggested, for example, that alternate mistuning may be nearly optimal in increasing the stability of shroudless fans. In this first section, an appropriate criterion for optimal mistuning will be defined and typical optimal mistuning patterns examined. In the next section, the mechanisms and limitations of mistuning will be discussed.

The selection of a definition of an optimal mistuning pattern is of course necessarily subjective. One must determine how to weigh the unlike quantities of stability, mistuning level, and forced response of the rotor. One choice is to implement the level of mistuning as a cost function to be minimized, and the desired level of stability of the least stable eigenmode as a constraint. Hence, the optimal mistuning problem can be posed as a constrained optimization problem.

The cost function which represents the level of mistuning in the rotor should of course strongly penalize large amounts of mistuning in any single blade. The cost function used by Crawley and Hall (1985) is given by

$$\varphi = \left[\frac{\sum \epsilon_i^n}{N}\right]^{1/n} \qquad (90a)$$

where n is in general some positive integer. In particular, n was chosen to be 4. Since this cost strongly penalizes large amounts of mistuning in any single blade, no blade mistuning becomes excessively larger than that of any other blade. That is to say that there will be no "rouge blades" in the optimal mistuning pattern.

The designer of a fan might wish to specify that a fan have at its operating point some minimum stability level. Hence the stability requirements are simply that the damping ratio of every eigenmode of the mistuned fan be greater than some minimum damping ratio. This is expressed symbolically as

$$\theta_i = \zeta_i - \bar{\zeta} \geq 0 \quad i=1,2,\cdots,N \qquad (91)$$

where ζ_i is the damping ratio of the ith eigenvalue, and $\bar{\zeta}$ is the desired stability margin. This requirement is shown graphically in Figure 6.

At this point, the optimization statement has been completely specified. The cost function to be minimized is a measure of the level of mass mistuning to be introduced into the rotor while the constraints are that the rotor meet minimum stability requirements. The independent variables are the individual mass mistuning of the blades or stiffness and the governing system equation is equation (63). This problem can be solved using appropriate numerical optimization techniques.

To illustrate the results of optimal mistuning, consider a specific high bypass ratio shroudless fan. The aeroelastic behavior is modelled using a typical section analysis by assuming a single torsional degree of freedom per blade. At this typical section, the relative Mach number, M, is 1.317; the reduced frequency, k, is 0.495; the solidity, is 1.404; the mass ratio, is 182; and the nondimensional radius of gyration, r, is 0.4731. Because the computational difficulty of the optimization problem rises quickly as the number of blades increases, the number of blades of the fan was taken to be 12, 13, or 14.

The unsteady aerodynamic model used is the supersonic linearized model of Adamczyk and Goldstein (1978). The aerodynamic influence coefficients found from this model are shown in Figure 9. Note that $Im(L_0)$ is less than zero indicating that the blades are self-damped. Hence, although the tuned rotor is unstable, mistuning may stabilize the rotor as previously discussed. Figure 9 also shows that the neighboring blades and the blade itself exert the dominant forces on a given blade. Therefore, the aerodynamic influence coefficient matrix is strongly banded.

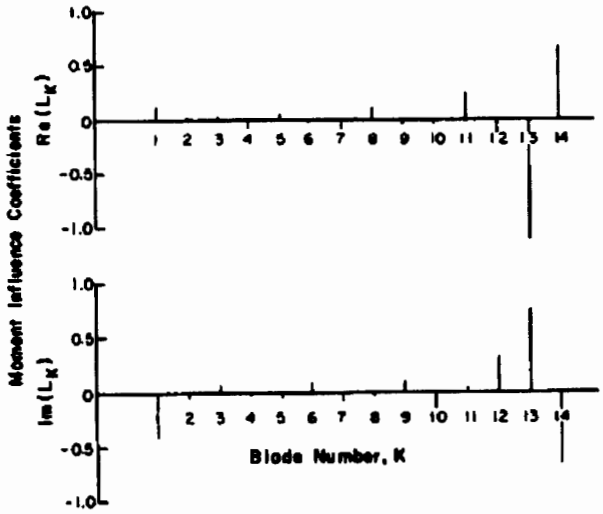

Figure 9. Unsteady Aerodynamic Moment Coefficients Showing the Influence of the i-th Blade on the 14th Blade in a 14-Bladed Rotor

Figure 10 shows the eigenvalues of the 14-bladed tuned rotor in nondimensional form. Note that four of the 14 eigenvalues lie in the right half plane and are therefore unstable. Since the blades are self-damped, the centroid of the eigenvalues lies in the left half plane.

Next the rotor is optimally mistuned by numerically finding a mistuning pattern which minimizes the cost function and satisfies all the constraints. Figure 11 shows the cost of the optimal mistuning pattern versus the desired amount of stability margin for the 12, 13, and 14-bladed cases. Also shown is the cost of alternate mistuning for the 14-bladed case. Two important points are clearly illustrated. First, although it has been previously thought that alternate mistuning may be nearly optimal (in the sense that a small amount of mistuning is necessary) this is not the case. For a desired damping ratio of 0.002, alternate mistuning requires nearly twice the level of mistuning as optimal mistuning. Second, it appears that the number of blades on the rotor is unimportant when optimally mistuning the rotor, and also that the optimal cost for 12, 13, and 14-bladed rotor are very similar.

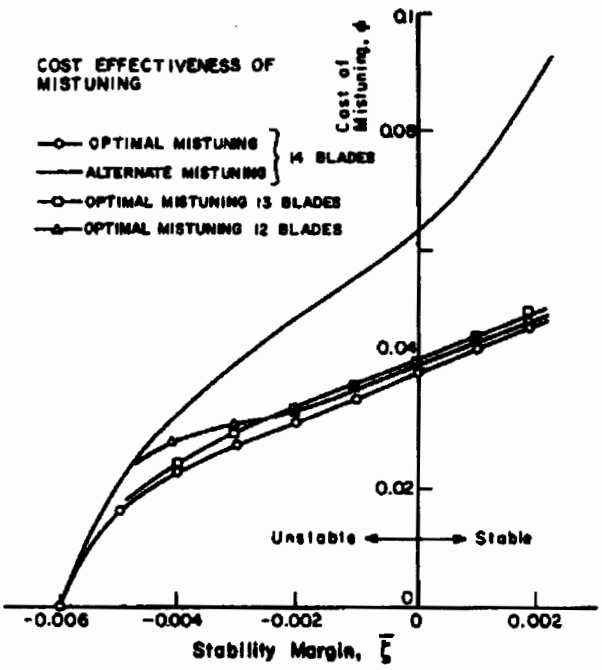

Figure 11. Cost of Mistuning for 12, 13, and 14-Bladed Rotors

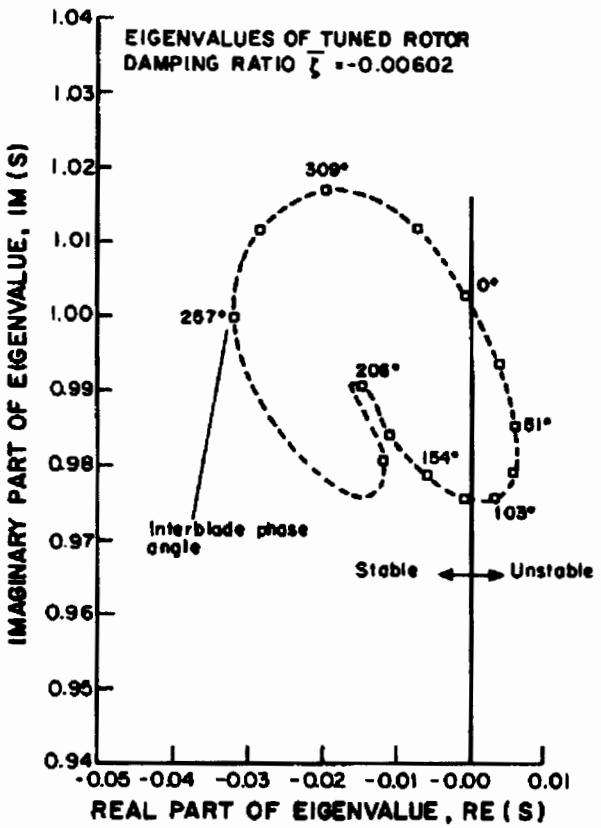

Figure 10. Eigenvalues of a Tuned Rotor

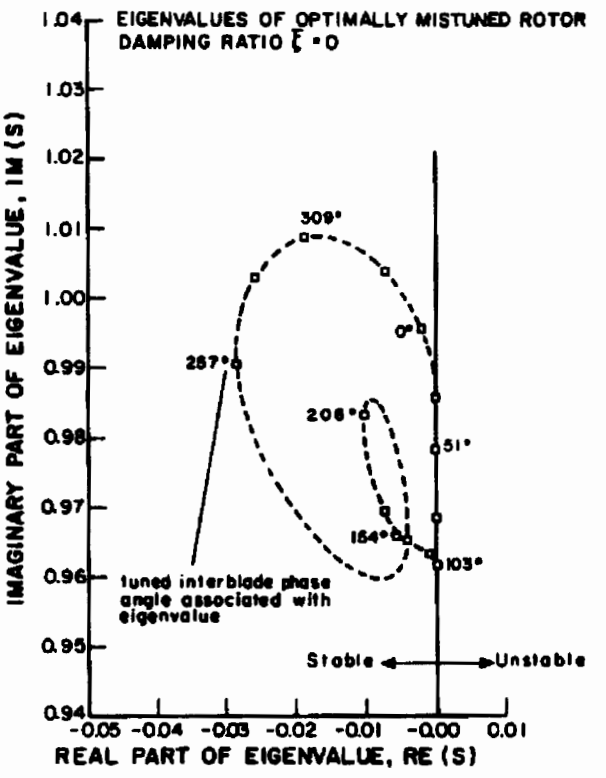

Figure 12. Eigenvalues of Optimally Tuned Rotor $\bar{\zeta}$=0

Mechanisms and Limitations of Mistuning

Some insight into why mistuning is effective can be gained by examining the eigenvalues of the tuned and mistuned rotors in the complex plane. Figures 10, 12, and 13 show the eigenvalues for the tuned case and the $\zeta = 0.0$ and the $\zeta = 0.002$ optimally mistuned cases for the 14-bladed rotor. As mistuning is introduced the eigenvalues are "pushed" to the left as much as necessary to satisfy the constraints.

The optimal mistuning patterns found in the optimization procedure for the 14-bladed rotor are shown in Figure 14. Beginning with the $\zeta = -0.005$, the pattern of mistuning is "almost alternate" mistuning. The odd numbered blades have little or no change from their nominal mass. As the stability margin is increased, the nearly alternate blade mistunings become more and more apparent.

Upon examination of a number of optimal mistuning patterns such as these, certain characteristic trends become apparent. An almost alternate pattern is evident which serves to reduce the dominant influence of the neighboring blades. This almost alternate mistuning pattern, however, is usually broken at one or two points around the rotor. It is thought that these breaks disrupt the communication of longer "wavelength" forces, that is, the smaller but nonzero influence coefficients from non-neighboring blades.

Finally, there is a certain fine structure to the mistuning pattern. The details of this structure depend on the details of the minimization, and it is difficult to predict what this structure will look like without actually performing the numerical optimization.

Unfortunately, the strict optimal mistuning pattern is sensitive to errors in implementation. Although the designer may specify a certain mistuning pattern, the manufacturing process may place limits on the tolerances which can actually be achieved. Hence, it is necessary to consider the sensitivity of a given mistune pattern to errors in implementation. For instance, if one wishes to implement an optimal mistune pattern on an actual rotor, the actual mistuning pattern which is implemented will be given by

$$\underset{\sim}{\varepsilon}_1 = \underset{\sim}{\varepsilon}_{1_{\text{specified}}} + \underset{\sim}{\varepsilon}_1 \qquad (92)$$

where e_i is the error in mistuning the rotor. The stability of this actual pattern may be significantly less than the one desired, depending on the errors introduced.

To investigate this problem, errors were introduced into the optimally mistuned 14-bladed rotor with a stability margin of 0.002. The procedure was to compute the worst case arrangement of the error and then assess the degradation in stability due to that case.

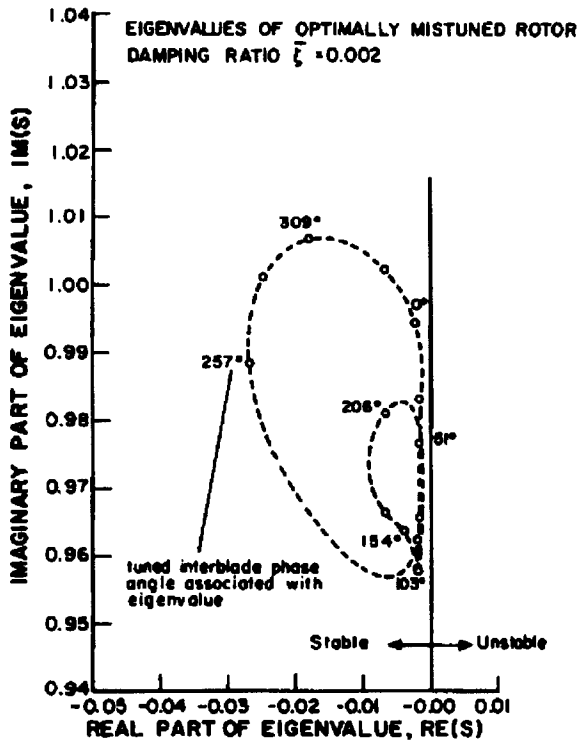

Figure 13. Eigenvalues of Optimally Tuned Rotor
$\bar{\zeta} = 0.002$

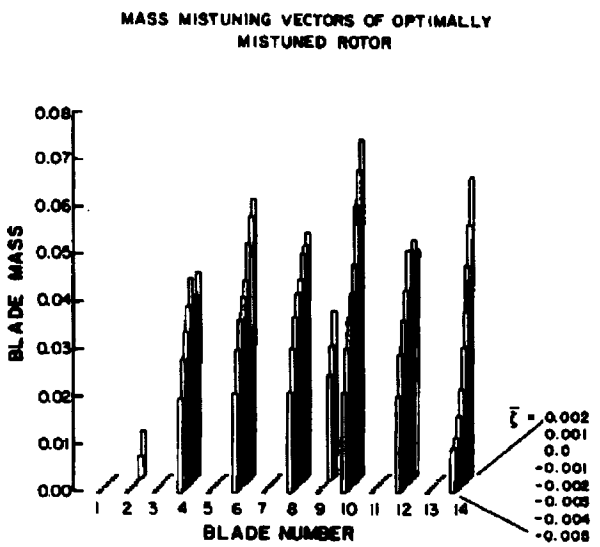

Figure 14. Optimum Mistuning Patterns of 14-Bladed Rotor

For an RMS scatter of 1 percent in mass mistuning, it was found that the stability was reduced from 0.002 to -0.00317 (Figures 15 and 16). The optimally mistuned rotor is extremely sensitive to errors in mistuning.

Hence we have seen that even though the optimal mistuning is the best possible mistuning pattern in one sense, that is, it requires the lowest level of mistuning to achieve a desired level of stability, it is clearly not practical to implement a pattern of mistuning which requires very close tolerances on the natural frequencies of the blades. As an alternative, consider the case of alternate mistuning. As was shown earlier, this mistune pattern is not nearly as effective as the optimal mistuning in terms of required levels of mistuning. However, the pattern is not as susceptible to errors in implementation as the optimal mistuning pattern. The same sensititivy analysis was applied to an alternately mistuned rotor with a perfectly mistuned stability margin of 0.00171. For a 1 percent RMS scatter in mass mistuning, the stability margin was reduced from 0.00171 to 0.00047 as shown in Figure 16. Therefore, although alternate mistuning is not as cost effective as optimal mistuning, it is clearly much more robust to errors in implementation.

Some insight into this difference in sensitivity can be gained by examining the trends shown in Figure 16. These trends can be divided into three regions. For the first few percent of mistuning introduced into the tuned rotor, very little change in stability occurs. In fact, it can be shown that for the first increment of mass mistuning of blades with a single degree of freedom, no change in stability occurs. Thus, on average, a rotor must have several percent mistuning before it begins to exhibit the behavior of a mistuned rotor.

Beyond the first few percent in mistuning, the trend enters an approximately linear region of sensitivity, that is, linearly increasing stability with increasing mistuning. Beyond this region, one moves into a region of diminishing returns. Eventually, the asymptotic limit of stability, the centroid of the eigenvalues, is approached and the level of mistuning required per increase in stability rises sharply.

This idealized trend can be used to explain the sensitivity of the optimum mistuning patterns. Figure 9 shows that the optimum cost curve has a very shallow slope in the region of $\zeta = 0.002$. This implies that a small amount of mistuning, if introduced correctly, can greatly increase the stability of the rotor. But for the same reason, small errors in mistuning can cause large decreases in stability. On the other hand, alternate mistuning is relatively insensitive to errors in mistuning but is not nearly optimal. Thus there is a clear design trade-off between the level of mistuning and the robustness of the design.

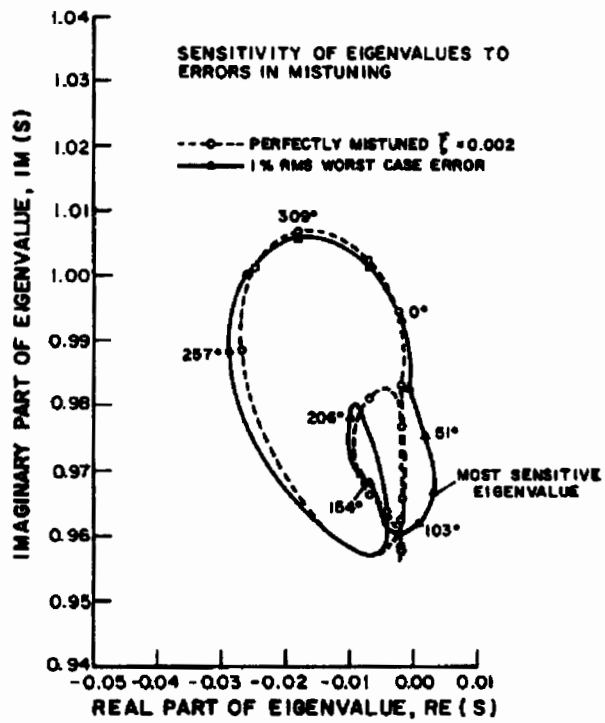

Figure 15. Sensitivity of Optimally Mistuned Eigenvalues to Errors in Mistuning

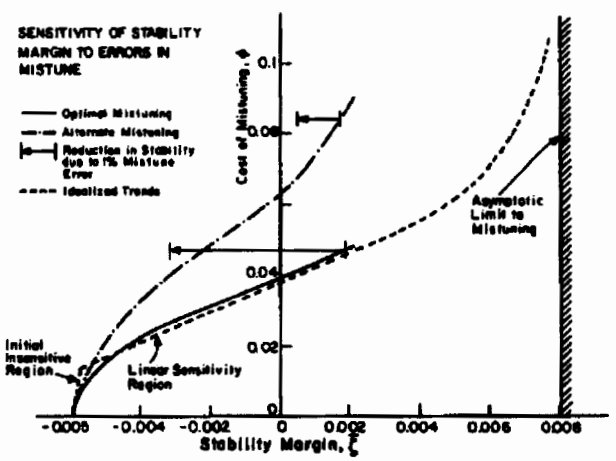

Figure 16. Sensitivity of Stability Margin to Errors in Mistuning

Summary Comments

In this chapter an attempt has been made to outline a complete and generalized formulation for the aeroelastic problem and its solution. This includes information necessary conventions of the aerodynamic and structural dynamic operators. The most important lesson to be learned from this review is that in the case of linear analysis, all of these analyses are equivalent, and the practicing engineer should use the one which gives the most insight into a particular problem.

In addition, a brief review of the most common trends in stability analysis was conducted: the destabilizing influences in cascades, the influence of kinematic vs. dynamic bending torsion coupling, the effects of mistuning, and the yet largely unmodelled effects of three-dimensionality.

Much of what has been presented in this chapter, except for the treatment of explicit time dependent motion in a cascade, exists in fragments distributed throughout the literature. But, here an attempt has been made to unite all of this material in a common formulation, and reference it to the remaining chapters of this Manual.

APPENDIX A: SUMMARY OF TRANSFORMATION RELATIONSHIPS

Basic relationships (for single degree of freedom per blade):

Structural dynamics:

$$[M]\{\ddot{q}_1\} + [K]\{q_1\} = \{f_1\} \tag{A1}$$

Unsteady aerodynamics:

$$f_1 = \pi\rho b^2\omega^2 \sum_{n=0}^{N-1} \ell_{\beta_n} \bar{q}_{\beta_n} e^{j(\omega t + i\beta_n)}$$

$$\{f_1\} = \pi\rho b^2\omega^2 [E]\left[\ell_{\beta_n}\right]\left\{\bar{q}_{\beta_n}\right\} e^{j\omega t} \tag{A2}$$

Kinematics:

$$\{q_1\} = [E]\left\{\bar{q}_{\beta_n}\right\} e^{j\omega t} = \left\{\bar{q}_1\right\} e^{j\omega t} \tag{A3}$$

For blade coordinates:

transform equation 2 using equation 3

$$-\omega^2[M]\{\bar{q}_1\} + [K]\{\bar{q}_1\} = \{f_1\} = \pi\rho b^2\omega^2[E]\left[\ell_{\beta_n}\right][E]^{-1}\{\bar{q}_1\} \tag{A4}$$

For travelling wave coordinates:

transform equation 1 using equation 3

$$-\omega^2[E]^{-1}[M][E]\left\{\bar{q}_{\beta_n}\right\} + [E]^{-1}[K][E]\left\{\bar{q}_{\beta_n}\right\} = \pi\rho b^2\omega^2\left[\ell_{\beta_n}\right]\left\{\bar{q}_{\beta_n}\right\} \tag{A5}$$

For standing mode coordinates (sin/cos):

transform eqn. 4 for q_1 and premultiply by $[P]^{-1}$

$$-\omega^2[P]^{-1}[M][P]\begin{bmatrix}\bar{q}_{cn}\\ \bar{q}_{sn}\end{bmatrix} + [P]^{-1}[K][P]\begin{bmatrix}\bar{q}_{cn}\\ \bar{q}_{sn}\end{bmatrix} = \pi\rho b^2\omega^2[P]^{-1}[L][P]\begin{bmatrix}\bar{q}_{cn}\\ \bar{q}_{sn}\end{bmatrix} \tag{A6}$$

For standing mode coordinates (general):

transform eqn. 4 for q_1 and premultiply by $[\phi]^T$

$$-\omega^2[\phi]^T[M][\phi]\left\{\bar{q}_n\right\} + [\phi]^T[K][\phi]\left\{\bar{q}_n\right\} = \pi\rho b^2\omega^2[\phi]^T[L][\phi]\left\{\bar{q}_n\right\} \tag{A7}$$

Other useful transformation relationships:

$$q_1 = \mathrm{Re}\left\{\left[\bar{q}_{co} + \sum_{n=1}^{(N-1)/2} \bar{q}_{cn}\cos n\theta_1 + \sum_{n=1}^{(N-1)/2} \bar{q}_{sn}\sin n\theta_1\right] e^{j\omega t}\right\}$$

$$\left\{\bar{q}_1\right\} = [P]\begin{bmatrix}\bar{q}_{cn}\\ \bar{q}_{sn}\end{bmatrix}$$

$$\begin{bmatrix}\bar{q}_{cn}\\ \bar{q}_{sn}\end{bmatrix} = \begin{bmatrix}\bar{q}_{co}\\ \bar{q}_{c1}\\ \bar{q}_{s1}\\ \bar{q}_{c2}\\ \bar{q}_{s2}\\ \vdots\end{bmatrix}$$

$$[P] = \begin{bmatrix} C_{0,0} & C_{0,1} & S_{0,1} & C_{0,2} & S_{0,2} & \cdots \\ C_{1,0} & C_{1,1} & S_{1,1} & C_{1,2} & S_{1,2} & \cdots \\ C_{2,0} & \vdots & \vdots & \vdots & \vdots & \\ C_{3,0} & & & & & \\ \vdots & & & & & \\ C_{N-1,0} & \cdots & & & & \end{bmatrix}$$

where $C_{k,\ell} = \cos 2\pi\frac{k\ell}{N}$ and $S_{k,\ell} = \sin 2\pi\frac{k\ell}{N}$

$$[P]^T[P]=[D]=\begin{bmatrix} N & & & & 0 \\ & N/2 & & & \\ & & N/2 & & \\ & & & N/2 & \\ 0 & & & & \ddots \end{bmatrix}, \quad [P]^{-1}=[D]^{-1}[P]^T$$

$$q_i = \mathrm{Re}\left\{\sum_{n=0}^{N-1} \bar{q}_{\beta_n} e^{j(\omega t + \beta_n i)}\right\}$$

$$\left\{\bar{q}_i\right\} = [E]\left\{\bar{q}_{\beta_n}\right\}$$

$$[E] = \begin{bmatrix} E_{0,0} & \cdots & E_{0,N-1} \\ \vdots & & \vdots \\ E_{N-1,0} & \cdots & E_{N-1,N-1} \end{bmatrix} \qquad E_{k,\ell} = e^{j\frac{2\pi k\ell}{N}} \qquad E^{-1}_{k,\ell} = \frac{1}{N} e^{-j\frac{2\pi k\ell}{N}}$$

$$[E]^{-1}[P]\begin{bmatrix} \bar{q}_{cn} \\ \bar{q}_{sn} \end{bmatrix} = \left\{\bar{q}_{\beta_n}\right\}$$

$$[E]^{-1}[P] = \begin{bmatrix} 1 & 0 & 0 & 0 & 0 & 0 & 0 & \cdots \\ 0 & \frac{1}{2} & -\frac{1}{2}j & 0 & 0 & 0 & 0 & \cdots \\ 0 & 0 & 0 & \frac{1}{2} & -\frac{1}{2}j & 0 & 0 & \cdots \\ \vdots & \vdots & \vdots & \vdots & \vdots & \vdots & \vdots & \\ 0 & 0 & 0 & \frac{1}{2} & \frac{1}{2}j & 0 & 0 & \cdots \\ 0 & \frac{1}{2} & \frac{1}{2}j & 0 & 0 & 0 & 0 & \cdots \end{bmatrix}$$

APPENDIX B: FORCE AND MOMENT NOTATION

Force notation usually used with the C_η notation

The forces and moments are initially defined to be acting at the leading edge (see figure 3b), and the displacements and wake velocities are:

$\tilde{q}_0 e^{j\omega t}$: leading edge velocity
$\tilde{\alpha}_0 e^{j\omega t}$: angular displacement
$\tilde{w}_0 e^{j\omega t}$: wake velocity at leading edge

The forces and moments acting at the leading edge are:

$$\tilde{F}_0 = \pi\rho Uc(C_{Fq}\cdot\tilde{q}_0 + U\cdot C_{F\alpha}\cdot\tilde{\alpha}_0 - C_{Fw}\cdot\tilde{w}_0)\cdot e^{j\omega t} \qquad \text{(B1a)}$$

$$\tilde{M}_0 = \pi\rho Uc^2(C_{Mq}\cdot\tilde{q}_0 + U\cdot C_{M\alpha}\cdot\tilde{\alpha}_0 - C_{Mw}\cdot\tilde{w}_0)\cdot e^{j\omega t} \qquad \text{(B1b)}$$

If the axis of pitch is shifted to a point ηc behind the leading edge, the coefficients about this axis (designated by subscript η) are derived by considering the transformation in coordinates and forces:

$$\tilde{q}_\eta e^{j\omega t} = \tilde{q}_0 e^{j\omega t} + \eta c\frac{d}{dt}(\tilde{\alpha}_0 e^{j\omega t})$$
$$\tilde{\alpha}_\eta e^{j\omega t} = \tilde{\alpha}_0 e^{j\omega t} \qquad \tilde{F}_\eta = \tilde{F}_0$$
$$\tilde{w}_\eta e^{j\omega t} = \tilde{w}_0 e^{-j\lambda\eta} e^{j\omega t} \qquad \tilde{M}_\eta = \tilde{M}_0 - \eta c\cdot\tilde{F}_0$$

where $\eta = 0$ at the leading edge, 1 at the trailing edge, and $\lambda = \omega c/U$. The new coefficients are:

$$\begin{aligned} (C_{Fq})_\eta &= (C_{Fq})_0 \\ (C_{F\alpha})_\eta &= (C_{F\alpha})_0 - j\lambda\eta(C_{Fq})_0 \\ (C_{Fw})_\eta &= e^{j\lambda\eta}(C_{Fw})_0 \\ (C_{Mq})_\eta &= (C_{Mq})_0 - \eta(C_{Fq})_0 \\ (C_{M\alpha})_\eta &= (C_{M\alpha})_0 - \eta(C_{F\alpha})_0 - j\lambda\eta(C_{Mq})_0 + j\lambda\eta^2(C_{Fq})_0 \\ (C_{Mw})_\eta &= e^{j\lambda\eta}(C_{Mw})_0 - \eta e^{j\lambda\eta}(C_{Fw})_0 \end{aligned} \qquad \text{(B2)}$$

$$\tilde{F}_\eta = \pi\rho Uc[(C_{Fq})_\eta\cdot\tilde{q}_\eta + U(C_{F\alpha})_\eta\cdot\tilde{\alpha}_\eta - (C_{Fw})_\eta\cdot\tilde{w}]\cdot e^{j\omega t} \qquad \text{(B3a)}$$

$$\tilde{M}_\eta = \pi\rho Uc^2[(C_{Mq})_\eta\cdot\tilde{q}_\eta + U(C_{M\alpha})_\eta\cdot\tilde{\alpha}_\eta - (C_{Mw})_\eta\cdot\tilde{w}]\cdot e^{j\omega t} \qquad \text{(B3b)}$$

Force Notation used with the ℓ notation

The forces and moments are assumed to be acting at the elastic axis (see figure 3a), and the displacements and wake velocities are,

$h = \bar{h}\cdot e^{j\omega t}$: displacement of the reference axis
$\alpha = \bar{\alpha}\cdot e^{j\omega t}$: angular displacement
$w = \bar{w}\cdot e^{j\omega t}$: wake velocity of the reference axis

And the forces and moments are written as:

$$\frac{L}{b} = \pi\rho b^2\omega^2\left(\ell^{hh}\cdot\frac{\bar{h}}{b} + \ell^{h\alpha}\cdot\bar{\alpha} + \ell^{hw}\cdot\frac{\bar{w}}{U}\right)\cdot e^{j\omega t} \qquad \text{(B4a)}$$

$$\frac{M}{b^2} = \pi\rho b^2\omega^2\left(\ell^{mh}\cdot\frac{\bar{h}}{b} + \ell^{m\alpha}\cdot\bar{\alpha} + \ell^{mw}\cdot\frac{\bar{w}}{U}\right)\cdot e^{j\omega t} \qquad \text{(B4b)}$$

By comparison of the two conventions,

$$\begin{aligned} \tilde{F}_\eta &= L \\ \tilde{M}_\eta &= -M \\ q_\eta &= -\frac{d\bar{h}}{dt} = -j\omega\cdot\bar{h} \\ \tilde{\alpha}_\eta &= -\bar{\alpha} \\ \tilde{w}_\eta &= -\bar{w} \\ c &= 2b \end{aligned}$$

and with these conventions:

$$\ell^{hh} = \frac{2i}{k}(C_{Fq})_\eta \qquad \ell^{mh} = \frac{4i}{k}(C_{Mq})_\eta$$
$$\ell^{h\alpha} = \frac{2}{k^2}(C_{F\alpha})_\eta \qquad \ell^{m\alpha} = \frac{4}{k^2}(C_{M\alpha})_\eta$$
$$\ell^{hw} = \frac{-2}{k^2}(C_{Fw})_\eta \qquad \ell^{mw} = \frac{-4}{k^2}(C_{Mw})_\eta$$